TURBINE BLADE TIP LEAKAGE LOSS INVESTIGATION

by

Ayman ABOU-SALEM

THESIS PRESENTED TO ÉCOLE DE TECHNOLOGIE SUPÉRIEURE
IN PARTIAL FULFILLMENT FOR A MASTER'S DEGREE
WITH THESIS IN AEROSPACE ENGINEERING
M.A.Sc.

MONTREAL, SEPTEMBER 20, 2016

ÉCOLE DE TECHNOLOGIE SUPÉRIEURE
UNIVERSITÉ DU QUÉBEC

ACKNOWLEDGMENT

ENQUÊTE SUR LES FUITES D'EXTRÉMITÉS D'AUBE DE TURBINES

Ayman ABOU SALEM

RÉSUMÉ

Bien que les méthodes actuelles pour évaluer le dégagement des extrémités d'aubes utilisent des corrélations expérimentales pour calculer les pertes et fuites d'aubes de la turbine, ces valeurs ont été jugées incompatibles et donc nécessitent des améliorations. Par exemple, les anneaux d'aubes carénées de la turbine avec des joints droits ont des pertes de dégagement des extrémités améliorées par rapport aux anneaux d'aubes carénés de la turbine avec des joints étagés. L'un des objectifs de cette étude actuel était d'enquêter sur la manière dont la géométrie de l'extrémité des aubes contribue à les pertes et fuites d'aubes dans une turbine en rapprochant les anneaux d'aubes carénés de la turbine qui ont plusieurs configurations, chacune ayant une combinaison du diamètre extérieur (DE) droit, DE étagée, d'ailettes verticales et d'ailettes inclinées. Le deuxième objectif était d'élaborer une corrélation pour les pertes de dégagement des extrémités améliorées, en comparant des corrélations entre les valeurs expérimentales existant avec les résultats du calcul de la mécanique des fluides numérique (MFN), récupéré après l'analyse de simulation. Plus particulièrement, les simulations MFN ont été effectuées sur plusieurs configurations d'une turbine des premiers étages (PT). Ces configurations différait l'un de l'autre en terme de la géométrie des extrémités d'aubes (p.ex., caréné avec une dérive inclinée, caréné avec deux dérives verticales) et une paroi d'enveloppe ou diamètre extérieur (p.ex., DE étroite, DE étagée) sur la zone de l'extrémité des aubes et ont été comparées selon ces caractéristiques. L'analyse de MFN était effectuée de tous les modèles et comportait le processus suivant : création de modèles CAD, étude du réseau, préparation des modèles pour maillage, et simulation MFN en exerçant les mêmes conditions limites. Une étude de l'indépendance par rapport à la grille a été effectuée sur une modèle pour vérifier la convergence de la grille. En raison de contraints de temps, des compromises ont été nécessaires et donc une dimension des ailettes d'environ 10 millions nœuds a été choisi. Toutes les configurations ont utilisées les mêmes paramètres pour la dimension des ailettes pour obtenir le même compte pour toutes les ailettes. Chaque configuration avait trois différents rapports portée-dégagement des extrémités d'aubes. Les résultats de la dynamique numérique des fluides a révélé que les configurations avec DE étagées avaient moins de pertes de dégagement des extrémités comparé aux configurations avec DE étroites. En outre, les ailettes verticales et les ailettes inclinées n'ont pas révélé une différence significative par rapport au flux de mass des extrémités d'aubes. La valeur de constant pour la corrélation expérimentale des pertes d'extrémités d'aubes a été modifié pour les configurations DE étagées et DE étroites en vue d'obtenir des nouvelles corrélations qui correspondaient aux efficacités d'analyse numériques de dynamique des fluides (MFN). Trois corrélations révisées des pertes d'extrémités d'aubes ont été acquises pour les configurations DE étroites, qui correspondaient à un, deux et trois ailette respectivement. D'autre part, pour les

configurations DE étagées, une seule corrélation révisée a été obtenu pour n'importe quel nombre de ailettes. Ces corrélations révisées, ont été implémentées dans l'outil *Pre-Detailed Design System (PDDS)*, qui est une conception des interfaces multi-préliminaire. En outre, ces corrélations améliorées ont été validées pour un design d'une aube de turbine de gaz. Des recherches plus poussées devraient vérifier les corrélations améliorées sur d'autres designs d'aubes.

Mots clés : dégagement des extrémités d'aubes, aubes carénés, DE étroite, DE étagée, ailette verticale et ailette inclinée

TURBINE BLADE TIP LEAKAGE LOSS INVESTIGATION

Ayman ABOU SALEM

ABSTRACT

Although current tip-clearance calculation methods utilize experimental-based correlations to calculate turbine tip leakage losses, these values have been found to be inconsistent and thus require improvement. For example, shrouded turbine blades with straight seals have better tip clearance loss than shrouded blades with stepped seals. One of the aims of this current study was to investigate the manner in which blade tip geometry contributes to tip leakage loss in a turbine by comparing shrouded blades that had several configurations, each of which has a combination of straight outer diameter (OD), stepped OD, vertical fins, and angled fins. The second aim was to develop an improved tip-clearance-loss correlation for straight seals, by comparing existing experimental-based correlations to Computational Fluid Dynamics (CFD) results retrieved following simulation analysis. More specifically, CFD simulations were performed on several configurations of a one-stage power turbine (PT). These configurations differed from each other in terms of blade tip geometries (e.g., shroud with one-angled fin, shrouded with two-vertical fins, etc.) and casing wall or outer diameter (i.e., straight OD, stepped OD) at the blade tip area and were compared based on these characteristics. CFD analysis of all models consisted of the following process: CAD model creation, grid study, mesh models preparation, and CFD simulation applying same boundary conditions. A grid independence study was performed on one model to check for grid convergence. Due to time constraints, a compromise needed to be reached and therefore, a mesh size of around 10 million nodes was chosen. All configurations used the same grid size parameters to obtain the same approximate grid count. Each configuration had three different tip-clearance-to-span ratios. CFD results from this study revealed that stepped OD configurations had less tip loss when compared to configurations with straight OD. In addition, angled and vertical fins did not reveal a significant difference (for stepped OD and straight OD configurations) in terms of tip mass flow. The constant value used in the tip loss experimental correlation was modified for stepped and straight OD configurations in order to obtain new correlations that matched efficiencies from CFD analysis. Three updated tip loss correlations were acquired for straight OD configurations, which corresponded to one, two, and three fins respectively. On the other hand, for stepped OD configurations, only one updated correlation was obtained for any number of fins. These updated correlations were implemented in the Pre-Detailed Design System (PDDS) tool, which is a multi-preliminary design interface. Furthermore, these improved correlations were validated for one blade design of a power turbine. Further research would need to verify these improved correlations on other blade designs.

TABLE OF CONTENTS

XII

LIST OF FIGURES

XIV

LIST OF ABREVIATIONS

CAD   Computer Aided Design

CFD   Computation Fluid Dynamics

LPT   Low Pressure Turbine

PSIO   Propulsion System Integration and Optimization

RANS   Reynolds-Averaged Navier-Stokes

RMSE   Root Mean Square Error

PDDS   Preliminary Multi-Disciplinary Optimization

RPM   Revolution Per Minute

BC   Boundary Condition

LIST OF SYMBOLS

Y Total Loss [%]

Y_p Profile Loss [%]

Y_s Secondary Loss [%]

Y_{TC} Tip Clearance Loss [%]

η_{tt} Total-to-total Stage Efficiency $[Dimensionless]$

$\Delta\eta$ Change in Total-to-total Stage Efficiency $[Dimensionless]$

φ Flow Parameter $\left[\frac{kg \cdot \sqrt{K}}{N \cdot S}\right]$

A Area $[m^2]$

W Mass Flow $\left[kg/s\right]$

T_U Seal Inlet Temperature $[K]$

P_U Seal Inlet Pressure $[Pa]$

P_D Seal Exit Pressure $[Pa]$

P_t Total Pressure at Vane Inlet (BC) $[Pa]$

T_t Total Temperature at Vane Inlet (BC) $[K]$

α Vane Inlet Angle (BC) $[Degrees]$

P_s Static Pressure at Blade Exit (BC) $[Pa]$

P_r Stage Pressure Ratio $= \frac{P_{exit}}{P_{inlet}}$ $[Dimensionless]$

P_{02Rel} Relative Pressure at Blade Inlet $[Pa]$

P_{03Rel} Relative Pressure at Blade Exit $[Pa]$

P_3 Total Pressure at Blade Exit $[Pa]$

γ Average Gas Ratio of Specific Heats $\left[\frac{J}{kg.K}\right]$

k' *Equivalent tip clearance for Shrouded Baldes* $= \dfrac{k}{(number\ of\ seals)^{0.42}}\ [inches]$

k *Tip Clearance* $[inches]$

c *True Chord* $[inches]$

h *Blade Span* $[inches]$

C_L *Airfoil Lift Coefficient* $[Dimensionless]$

s/c *Pitch to span Ratio* $[Dimensionless]$

α_1 *Relative gas angle at Blade Inlet* $[Degrees]$

α_2 *Relative gas angle at Blade Exit* $[Degrees]$

α_m *Mean gas angle* $= \tan^{-1}\left[\frac{1}{2}(\tan\alpha_1 - \tan\alpha_2)\right]\ [Degrees]$

INTRODUCTION

0.1 Background

Studying flow losses in gas turbines is a complex and challenging area of study in the field of aerospace; however, researchers have made immense efforts to understand the flow behavior in a gas turbine especially in complicated geometries. When air flows inside a power turbine for instance, it undergoes twists and turns around vanes and blades, and through the gap between the blade tip and casing. The combination of this 3-dimensional flow, complex blade shape and high rotational speed is the perfect environment for the initiation of losses. It has been found that due to pressure difference between the suction and pressure side in a turbine blade, the flow will tend to escape through the tip causing a disturbance in flow (Saravanamuttoo, et al., 2009). As a result, the clearance is kept as small as possible to minimize losses and can be estimated to be 1 to 2 percent of the average blade height (Saravanamuttoo, et al., 2009). This eventually will reduce the power generation and hence loss in efficiency. Therefore, finding ways to minimize the flow leakage at the tip of the rotor, through testing and validation of blade tip geometries with available resources and cost effective methods, has the potential to deliver a great value to the aerospace industry.

0.2 Frame Work

This study branches from the Industrial Research Chair (NSERC / P&WC), Propulsion System Integration and Optimization (PSIO) program, which is a conceptual tool created to integrate and automate gas turbine inputs in an efficient manner. The purpose of this program is to design gas turbines at a preliminary design stage and combine multi disciplines under the same tool, which is referred to as Pre-Detailed Design System (PDDS). As highlighted in **Figure 0-1**, the present work falls under the turbine aero calculation method. Following the completion of this study, updated tip loss correlations for stepped and straight outer diameter configurations were integrated within the PDDS. The PDDS tool can be divided into four

sections: (i) Knowledge Database, (ii) User Interface, (iii) Disciplines Involved, (iv) and Preliminary Results. These sections can be seen in **Figure 0-1** when looking at each row.
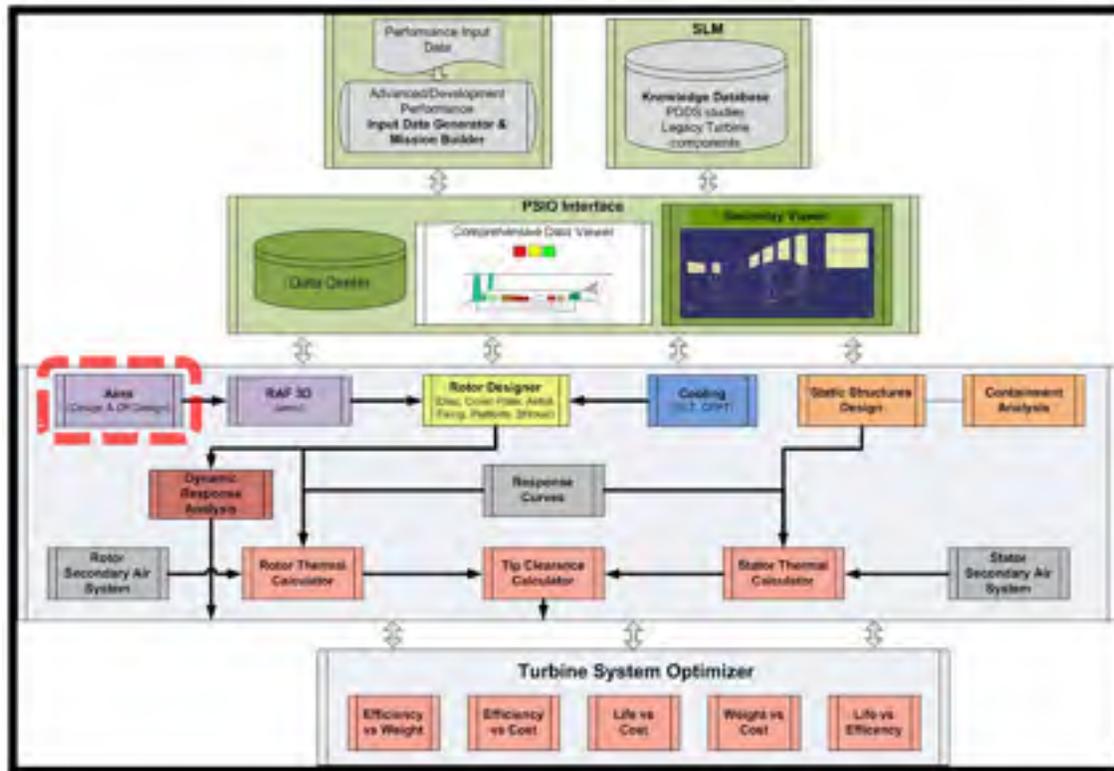
Figure 0-1 Pre-Detailed Design System (PDDS) High Level Map

The turbine aero mean-line tool is a one-dimensional analysis that performs calculations at the mid-span plane or passage between hub and tip of a vane or blade as shown in **Figure 0-1**. It summarizes thermodynamic properties such as temperatures, pressures and Mach numbers at several location across the turbine stage(s). In addition, turbine aero evaluates efficiencies and all losses including tip clearance loss in its output summary.
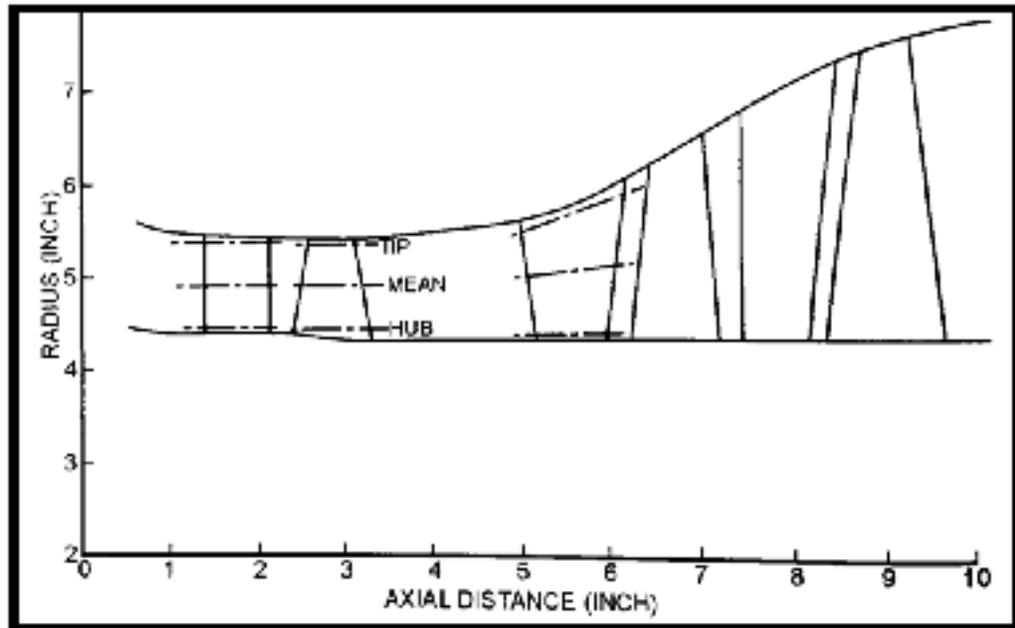
Figure 0-1 Mean-Line Plane (Moustapha, Zelensky, Baines, & Japikse, 2003)

Tip clearance loss is one of the primary and essential aerodynamic losses that require embedding within the PDDS tool. Understanding different blade tip designs and their impact on tip clearance loss is integral to evaluate gas turbine efficiency and assists with the prediction of the tip loss evaluation especially at a preliminary design level (Saravanamuttoo et al., 2009).

The theoretical underpinnings of current tip-loss evaluation techniques are rooted in mass flow correlations introduced by Vermes (1961) and Komotori & Miyake (1977). Inconsistencies in tip loss evaluation were identified when utilizing these mass flow correlations on turbine blades to evaluate tip loss. For example, straight seals showed better tip loss results than stepped seals. In addition, tip loss values did not decrease as number of fins increased. The current tip loss evaluation refers to the correlations used by the following three methods: Vermes, Komotori, and Vermes-Komotori's, without any citation. The mean-line tool lists the above three names as distinct methods used throughout the tip loss current evaluation. Although Vermes' (1961) and Komotori's (1977) individual papers were successfully identified in literature, no such paper was found wherein both Vermes and

Komotori appeared as co-authors. This is in contradiction to what the current mean-line tool quoted. Due to the lack of proper citation, it was not possible to verify the sources for further improvements and therefore, the alternative solution was to employ a relatively newer correlation by Kacker & Okapuu (1982).

Once Kacker & Okapuu's (1982) tip loss correlation was implemented in the mean-line code, the PDDS tool executes the code and subsequently calculates tip loss evaluation within a matter of seconds. Input needed for tip loss evaluation is blade tip type (shroud), number of fins (i.e. 1-, 2-, 3-fins) and tip clearance value, which can be easily dictated by one user. Ideally, with the completion of the PDDS tool, one user will be managing inputs from different disciplines and the aforementioned inputs needed for the tip loss evaluation can be keyed in with great ease.

0.3 Objective

The primary aim of this study was to expand upon tip loss correlation of shrouded blades, and to examine tip leakage of several blade tip configurations by simulating a one-stage (2nd stage) passage in an axial power turbine. The power turbine consists of two stages and only the second stage was chosen to simplify the studied model and to simulate without considering much of downstream effects. In addition, this research aimed to successfully update tip loss correlations obtained for straight OD configurations with one, two and three fins based on numerical simulation. Subsequently, the updated tip loss correlations were to be implemented within the mean-line code, which is a function performed by the PDDS tool. A final objective was to better understand flow behaviour, for different turbine blade tip-configurations using several fin types (angled, vertical) and outer diameter types (stepped, straight), in the zone in which interaction between blade tip and casing occurs.

CHAPTER 1

LITERATURE REVIEW

1.1 Overview

1.1.1 Aerodynamic Losses

Ideally, when designing blades in axial gas turbines, the gas flow is to be directed along the axial direction and at some parts, the tangential direction for work. In reality, this is not always the case because of the disturbance of the flow when it encounters curved surfaces such as vane or blade walls. This however, in addition to boundary effects and viscosity, will interrupt the flow streamlines and may cause flow separation, which is referred to as flow Aerodynamic losses.

Selection of the losses that occur in a typical blade passage are highlighted in **Figure 1-1, Figure 1-2** and **Figure 1-3**. These losses are divided into the following four types: *(i)* Profile loss (Y_p); *(ii)* Trailing edge loss (Y_t); *(iii)* Secondary loss (Y_s); and *(iv)* Tip clearance loss (Y_{TC}) (Moustapha, et al., 2003). This study focuses on the tip-clearance loss at several blade tip geometries.
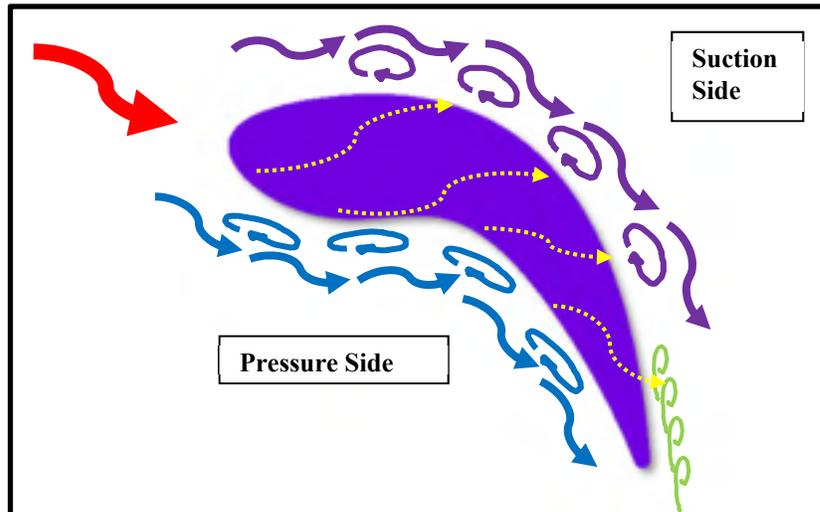
Figure 1-1 Blade Flow Losses Top View
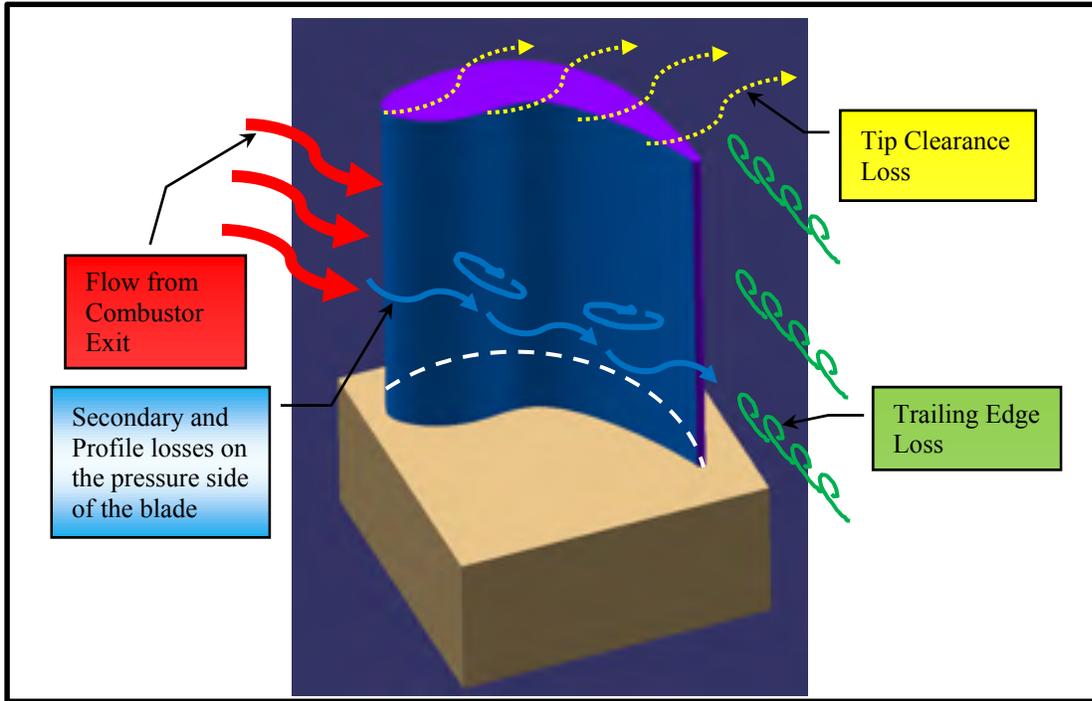
Figure 1-2 Blade Flow Losses Isometric View1
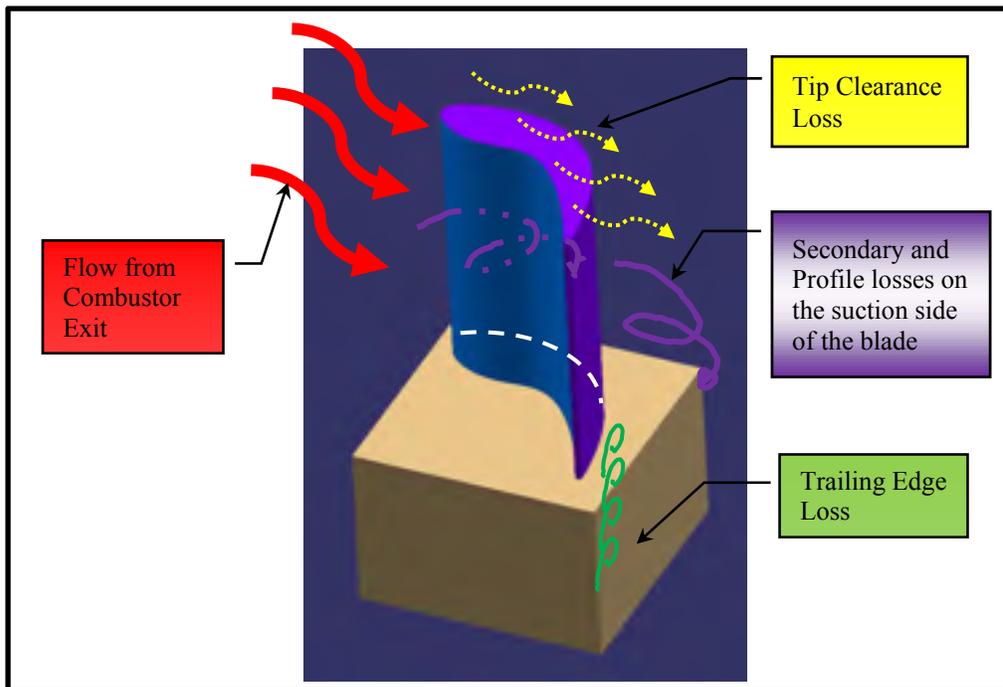
Figure 1-3 Blade Flow Losses Isometric View2

In practice, the total or overall blade losses can be expressed in terms of the profile loss, secondary loss and tip clearance loss as presented by in **equation (1-1)** (Saravanamuttoo, et al., 2009):

$$Total\ Blade\ Loss = Y = \frac{P_{02Rel} - P_{03Rel}}{P_{03Rel} - P_3}$$

$$= Y_p(Profile) + Y_s(Secondary) + Y_{TC}(Tip\ Clearance) \qquad (1\text{-}1)$$

Saravanamuttoo et al. (2009) mentioned that the secondary losses are a combination of the annulus losses and secondary flows such as trailing edge losses that exist when the wall boundary layer is subjected to turning by a neighboring rounded surface. **Figure 1-4** summarizes the breakdown of the total losses where the profile loss value is acquired directly from tests, and the values of the two components of the secondary losses are difficult to compute individually due to flow complexity (Saravanamuttoo, et al., 2009).
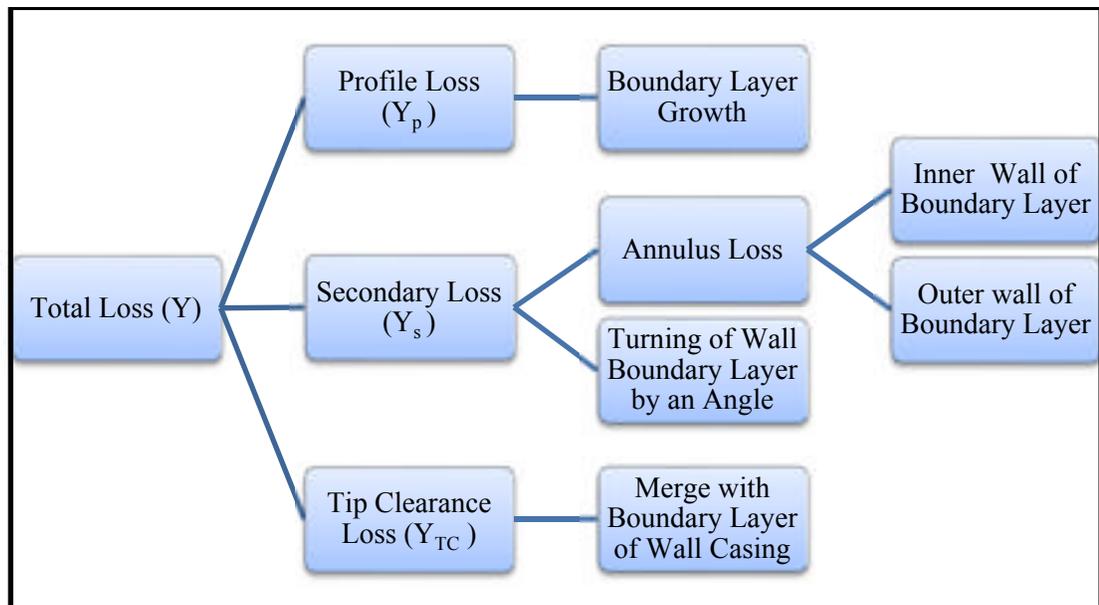
Figure 1-4 Total Loss Schematic

1.1.2   Tip Clearance Loss (Y_{TC})

Tip clearance loss arises solely in rotors (Moustapha, et al., 2003). Blades are mounted around the circumference of a disk, which is installed on a shaft, and they rotate for power extraction. In order that blades do not rub against the casing wall, a gap must be accounted for between the end of the blades and the wall. The term tip clearance refers to this gap, whereas tip clearance loss or tip leakage loss signifies the generation of vortices at this gap, which eventually causes loss in efficiency. Due to the pressure difference between the pressure and suction sides of the rotor, gas flows through the gap that separates the blade tip and the casing wall. This however, does not cause any significant work output (Moustapha, et al., 2003). The leakage flow between the moving blade and the stationary casing forms a tip leakage vortex, which is shown in **Figure 1-5**, where it is merged with secondary flow (Moustapha, et al., 2003).
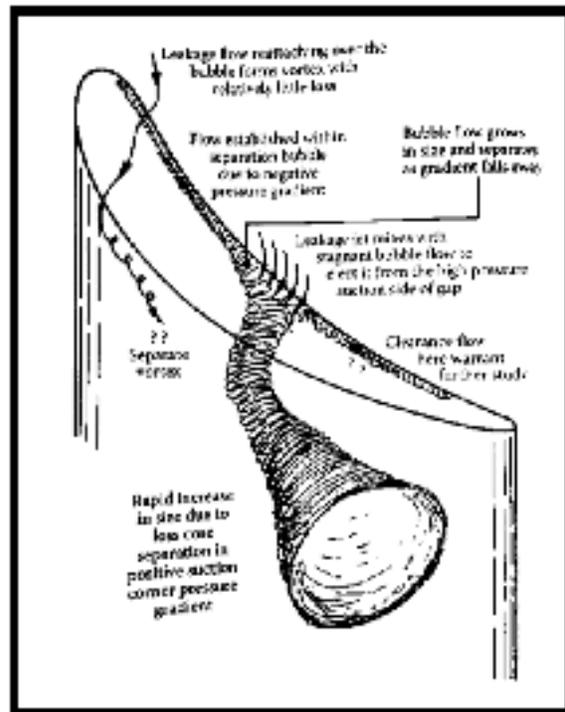
Figure 1-5 Tip Leakage Vortex at Rotor Tip
(Han, et al., 2013)

1.1.3   Tip Leakage Vortex Relation To Loss

A large number of studies agree that vortex effects, such as those generated over blade tip area, are directly linked to losses. An ASME journal article argued that vortex dynamics in tip clearance are of significant importance in determining tip losses (Huang, et al., 2013). Following performance of CFD simulation on different designs of unshrouded blades of an axial turbine, it was deduced that blade tip geometry and tip clearance value are associated with vortices breakdown, reversed flow, decrease of axial velocity (Huang, et al., 2013). Another doctoral thesis argued that vortices cause disturbances to the flow and make it unsteady, which causes a loss in efficiency and increase in vibration and noise (Intaratep, 2006). Therefore, it can be concluded that when vortices exist in a turbine, they cause disturbance to the flow as well as pressure drops and losses; this in turn contributes to loss in efficiency. The aforementioned studies, in addition to many others that investigate flow losses, consider the presence of vortices as a loss, which will be an assumption in this study.

1.1.4   Computation Fluid Dynamics (CFD) For Leakage Flow

With the ongoing advancement of computers, and the monumental increase in their power, speed, and storage, engineers have been able to perform complex calculations, such as simulating the flow inside a gas turbine, with greater ease in a virtual environment. Much research has been conducted to better understand the losses and flow behavior in a gas turbine using CFD software. One study utilized a CFD solver to investigate simple-type flow and time marching where a $K-\omega$ SST hybrid model was recommended to capture flow details (Tallman, 2002). Subsequent research has employed different approaches to understand losses, such as the mixing of plane and sliding mesh models using commercial finite-volume solver FLUENT (Shavalikul, 2009). Shavalikul (2009) implemented the circumferentially average mixing plane concept along with three turbulence models $K-\varepsilon$, $K-\omega$ and SST.   A recent study solved the standard Reynolds-Averaged Navier-Stokes (RANS) equations using ANSYS FLUENT CFD software as a way to investigate the loading

10

effects of tip leakage (Huang, et al., 2013). Saleh, et al. (2013) utilized numerical simulation (CFD software) to compare the experimental results of flow over flat and cavity blade tip-types. Research has also revealed that CFD software allows for the analysis and comparison of new blade-casing sealing concepts that are currently in use, such as tip labyrinth seal (Zhang, et al., 2014).

1.2   Earlier Blade Tip Geometries Studies

1.2.1   Un-Shrouded Blades With Multiple Clearance

An early correlational study by Patel (1980) concluded that when tip clearance was decreased to 0.88% of the blade height, the local efficiency showed the highest results to be approximately 92%, which is presented in **Figure 1-6**. Above 50% of span, a severe drop in the local efficiency is noticed, which is due to the increase of clearance-to-span ratio and tip-clearance-gap values (Moustapha, et al., 2003).
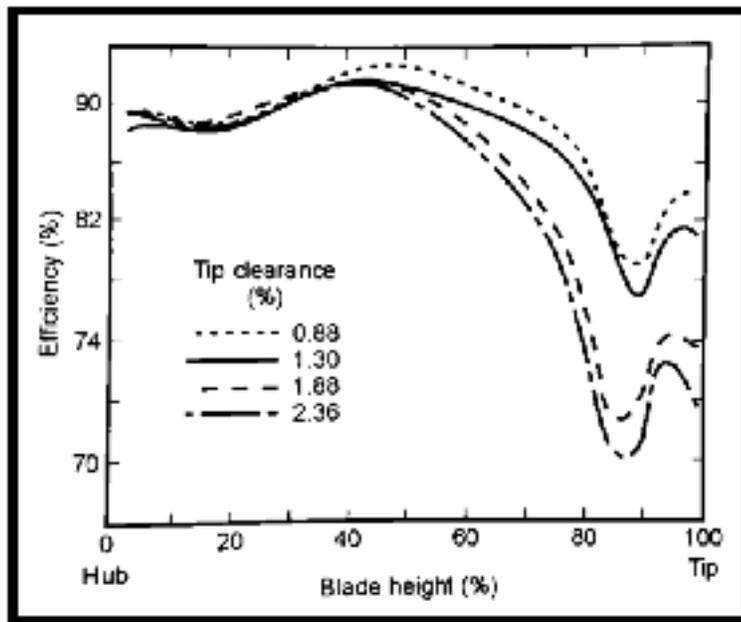
Figure 1-6 Tip Clearance to Blade Span Percentage
(Moustapha, et al., 2003)

1.2.2   Shrouded Blades With Stepped OD Seals With Angled Fins

The two main components of a seal are the outer wall and the fin (knife) as explained in **Figure 1-7**. The wall types can have a straight (horizontal) or a stepped geometry, whereas the fin has a straight (vertical) or angled geometry.
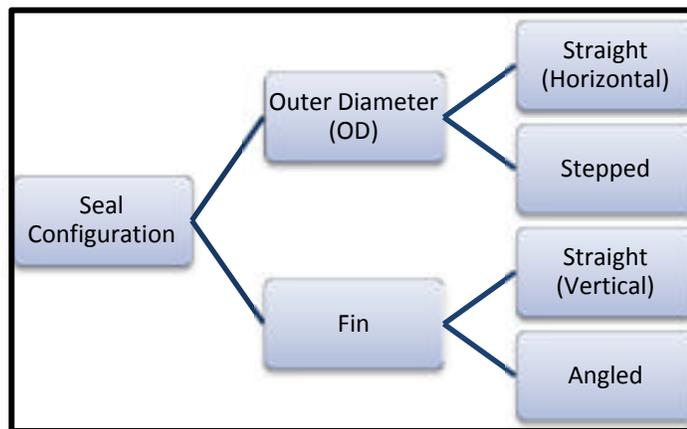
Figure 1-7 Seal Geometry Combination

Figure 1-8 is an example of an unconventional seal configuration that shows a divergent flow path. It consists of three angled fins against a stepped wall or outer diameter. When a seal's wall and fin(s) are straight, the seal is called a conventional labyrinth seal (Stocker, 1978).
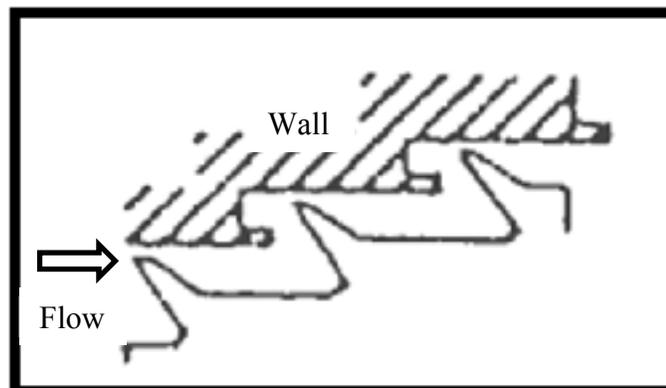
Figure 1-8 Three Angled-Fin Seal with Stepped Wall
(Stocker, 1978)

Stocker's (1978) experimental correlational study of seals aimed to reduce the seal leakage by improving seal effectiveness. Stocker (1978) studied several-stepped OD with angled seal designs and their tip leakage results were compared with conventional stepped seals with vertical fins.

According to Stocker (1978), stepped wall seals have lower leakage than straight-through OD seals, and seals with angled fins have better performance than seals with vertical fins. **Figure 1-9** shows the different designs prepared by Stocker (1978), which aimed to develop an optimized step seal configuration. Based on Stocker's experimental results, design 5 (similar to the stepped configuration used in this paper) showed the least tip leakage when compared to other designs and conventional step seals.
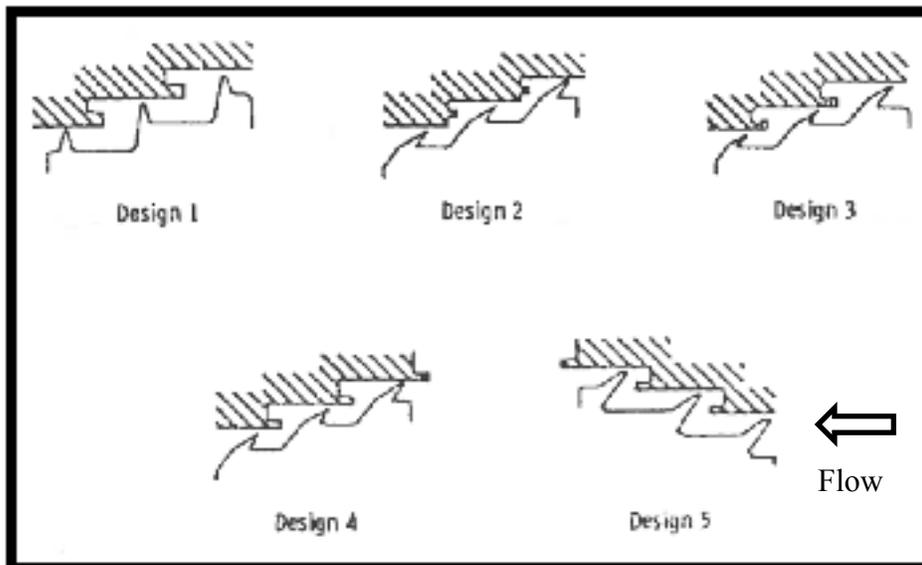
Figure 1-9 Seal Designs (Stocker, 1978)

Figure 1-10 presents the plots of flow parameters against the pressure ratios for all advanced designs along with the conventional seal. The performance range of the advanced designs is lower than conventional seal for the same pressure ratio; Stocker (1978) argued that advanced seal designs have the least leakage, with Design 5 results situated at the lower spectrum of this range shown in **Figure 1-10**. According to Stocker (1978), flow parameter

(φ) values are normally compared, for convenience, at a pressure ratio of 2.0. The flow parameter is directly proportional to the tip mass flow (W) and square root of the total upstream tip temperature (T_U), and inversely proportional to pressure upstream tip (P_U) (Stocker, 1978). The flow coefficient is a function of the mass flow, whereas seal pressure ratio is the ratio of upstream over downstream pressures at blade tip area.
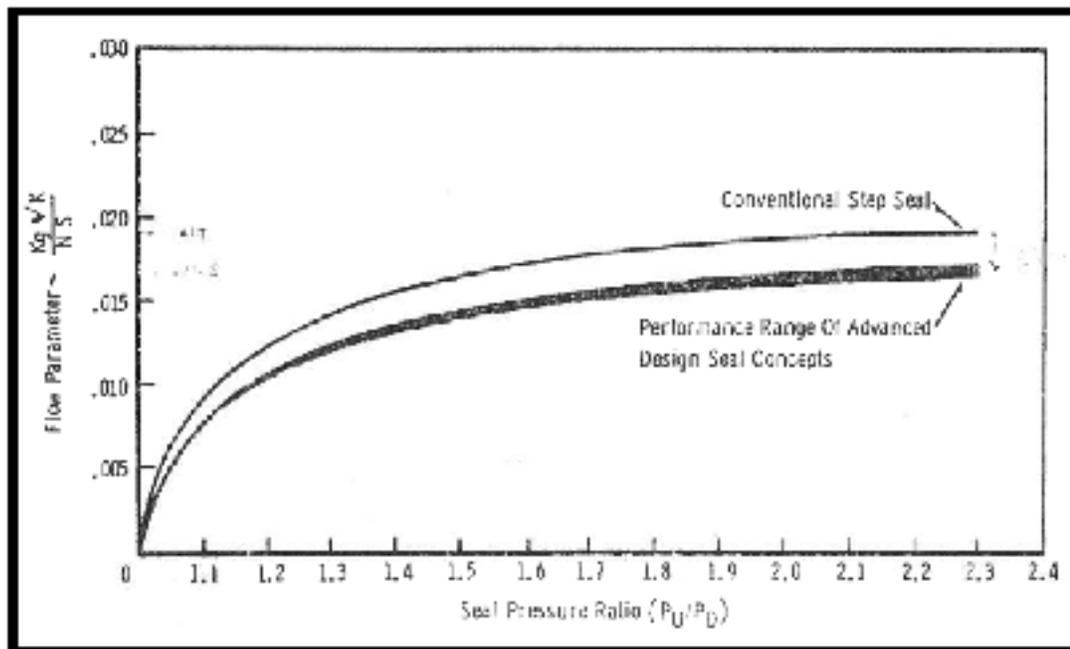
Figure 1-10 Advanced Seal Design (3-Finned Stepped) Performance (Stocker, 1978)

One of this study's aims was to validate that stepped OD configurations with angled fins contribute to less tip leakage loss as opposed to configurations with stepped OD and vertical fins. The larger the number of fins, the more resistance they add to tip flow; and hence, the smaller the tip leakage loss. In addition, configurations with stepped OD are expected to have less tip leakage loss than straight OD. Therefore, to confirm this hypothesis, CFD results must show that the 3-angled-fin blade tip configuration with stepped OD has the least tip leakage loss, whereas the 1-vertical-fin blade tip configuration with straight OD will show the highest tip leakage loss.

1.2.3   Tip Clearance Loss Correlation

Kacker & Okapuu (1982) presented a mean-line methodology that is capable of predicting the design point efficiencies of gas turbine engines; it included tip clearance loss calculations for unshrouded blades. Kacker & Okapuu (1982) also presented an experimental-based correlation for shrouded blades with straight seals. It was expressed as follows:

Shroud:
$$Y_{TC} = 0.37 \frac{c}{h} \left(\frac{k'}{c}\right)^{0.78} \left(\frac{C_L}{s/c}\right)^2 \frac{(\cos \alpha_2)^2}{(\cos \alpha_m)^3} \qquad (1\text{-}2)$$

Where

k' : *Equivalent tip clearance for Shrouded Blades* $= \dfrac{k}{(number\ of\ seals)^{0.42}}$ $\qquad (1\text{-}3)$

k : *Tip Clearance* [inches]

c :   *True Chord* [inches]

h :   *Blade Span* [inches]

C_L : *Airfoil Lift Coefficient*

s/c : *Pitch to span Ratio*

α_1 : *Relative gas angle at Blade Inlet*

α_2 : *Relative gas angle at Blade Exit*

α_m : *Mean gas angle* $= tan^{-1} \left[\frac{1}{2}(tan\ \alpha_1 - tan\ \alpha_2)\right]$ $\qquad (1\text{-}4)$

1.2.4   Blade Tip Structures And Impact On Flow

The relationship between flow and the structure of a blade tip has been validated throughout the existing body of research. Previous studies on tip leakage loss have found that when blade tip design is modified, tip losses vary accordingly (Camci, et al., 2005), (Zhou, Hodson, et al., 2013), (Szymański, et al., 2014) and (Yoon, et al., 2014). This variation depends specifically on tip geometries, which manipulate gas flow at the gap between the blade tip and casing wall. Existing literature in the field has also examined the performance of various blade tip designs under different operating conditions; ultimately concluding that

tip leakage loss depends on the boundary conditions of each study's set-up in terms of CFD simulation. The impact of blade tip geometry is summarized in this section by examining the key research findings from recent studies that investigated tip leakage.

A computational study by Tallman (2002), in which he investigated chamfering of the suction side edge, the pressure side rounded edge and the squealer-type tip cavity, found that the chamfering of the suction side edge reduced the tip leakage vortex but increased the secondary losses (Tallman, 2002). In addition, the study recommended against the rounding of the pressure side edge since this setup did not contribute to a reduction in tip leakage vortex (Tallman, 2002). Furthermore, the squealer-type blade tip was found to have a minimal impact on secondary flow and did not cause any losses at the tip gap (Tallman, 2002).

Camci et al. (2008) tested two types of squealer blade tips entitled Suction Channel (SqCh) and Suction Side Squealer (SSSq), which is exhibited at the left and right of **Figure 1-11** respectively. Each squealer type had several configurations that represented different designs, as indicated in the legend on the top row of the **Figure 1-11** (Camci, Dey, & Kavurmacioglu, 2005). The Suction Channel had two configurations, SqCh-A and SqCh-B, whereas the Suction Side Squealer had three configurations, SSSq-A, SSSq-B, and SSSq-C (Camci, Dey, & Kavurmacioglu, 2005).
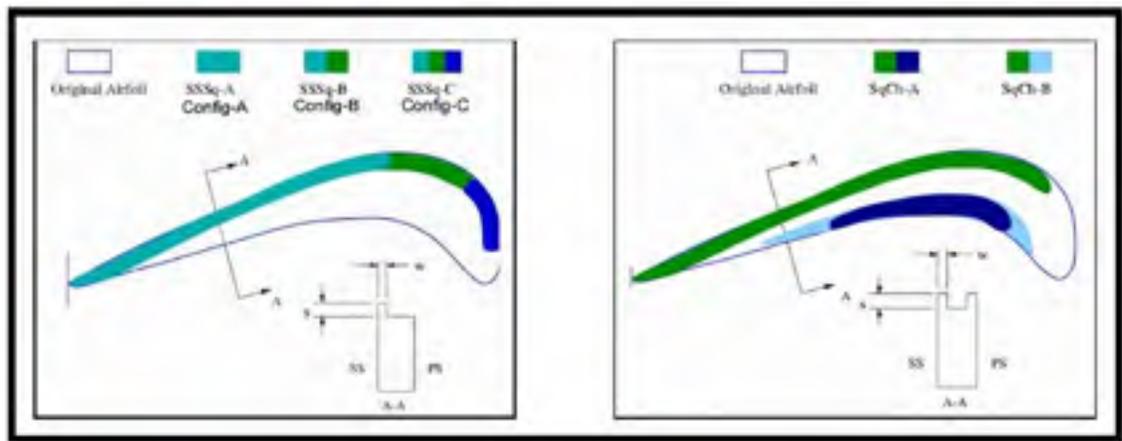
Figure 1-11 Blade Tip Geometry Employed by Camci
(Camci, et al., 2005).

The experimental study deduced that squealer seals were effective in reducing the tip leakage when the tip clearance to blade span ratio is about 0.72%; however, results showed that partial squealer seal configurations were more effective in terms of tip sealing than full squealer (Camci, et al., 2005). Furthermore, CFD results showed that Config-B showed better performance than that of Config-A and Config-C in reducing the tip leakage flow, where every tip profile had its optimal rim length for effective sealing (Camci, Dey, & Kavurmacioglu, 2005). In addition, the SqCh-B (longer rim on pressure side) configuration, when compared to the SqCh-A one, exhibited a minor difference for tip leakage flow (Camci, Dey, & Kavurmacioglu, 2005). Results indicated that Config-B was the most effective in reducing mass flow rate, and it was concluded that the rim on the pressure side did not have any effect in preventing the flow at the tip of the blade (Camci, Dey, & Kavurmacioglu, 2005).

Another recent study presented a numerical analysis of different tip seal (labyrinth seal) configurations using CFX software and K$-\omega$ SST turbulence model, 2.6M nodes; in an attempt to minimize turbulence intensity at the outlet area (Szymański, et al., 2014). The outcome of this study showed that when maximum surface roughness at the casing wall was taken into account, the relative mass flow dropped by 20.1% (Szymański, et al., 2014). The study also found that, in addition to the surface roughness of 50 μm, a 30-degree inlet angle was also a factor in reducing mass flow, which contributed to a drop of 31% of relative mass flow (Szymański, et al., 2014). CFD result comparison and validation with experimental results were part of the future work of this study (Szymański, et al., 2014). Zhou, Hodson, Tibbott and Stokes (2013) performed an experimental and numerical study of a winglet tip type and compared results to flat and cavity tip models. The study concluded that the tip leakage was reduced around the leading edge of blade tip, and was enhanced starting from mid-chord to the trailing edge (Zhou, et al., 2013).

The studies outlined throughout this section show the direct effect and relation between blade tip type and tip clearance losses. Each study focused on distinct aspects of the interaction between the blade tip and casing wall. This current research study will focus on

evaluating the tip loss of fully shrouded blades with up to three fins. Minimal research has been performed on fully shrouded blades with fin(s) seal-type; only one recent comparative study examined the sealing effects of shrouded blades (Yoon, Curtis, Denton, & Longley, 2014). It is expected that this study will confirm the premise that tip configurations have an impact on tip losses. More specifically, it is hypothesized that there will be a decrease in tip loss when tip configurations, with straight casing walls, are changed according to the subsequent order: shrouded with 1-, 2-, and 3-fin(s). Tip losses with a stepped casing wall will be compared to the shrouded blades with 1-, 2- and 3-fins with a straight wall set-up.

1.2.5   Labyrinth Seals

Numerous efforts have been made in previous research to investigate tip-leakage loss for various applications with different setups such as, tip wall with honeycomb type, brush seals type, nonrotating seals, etc. This study was an extension of previous tip-leakage loss research in that it investigated a one-stage model of an axial power turbine with different configurations at three tip-clearances each.

In a recent doctoral study, CFD analysis was performed on three configurations: stepped-up (convergent path), stepped-down (divergent path) and straight seals (Collins, 2007). Each configuration had four vertical-finned seals and a honeycomb outer diameter type (Collins, 2007). Collins (2007) prepared an experiment of the same configurations and compared data with numerical results, which revealed that tip seal performance was dependent on the fin location with respect to the OD groove. FLUENT and GAMBIT meshing software were utilized to create configurations with mesh sizes between 44,000 and 800,000 nodes, then simulation in CFX.

Li et al. (2012) presented a leakage study on a brush seal (nine fins, 6 short and 3 long) with four different rotational speeds and five pressure ratios for two-tip clearance. Li et al.'s (2012) results revealed that CFD simulation should account for rotor centrifugal growth, because this growth will decrease the tip clearance gap especially at high rotational speeds and therefore, will act as a better seal. Li, et al.'s (2012) study created mesh structures

(51,701 nodes) using ANSYS ICEM CFD and then imported to ANSYS FLUENT commercial software.

Gamal and Vance (2008) performed a series of nonrotating tests to investigate labyrinth seals of different configurations for high-pressure applications in turbomachines and found that increasing (doubling) the fin thickness influences leakage and reduces flow leakage by 20%. In addition, Gamal and Vance (2008) argued that beveled fins limit leakage at seal downstream, whereas vertical fins were better with tighter clearances.

An additional doctoral study performed an experimental tip loss study on a blade in a high-pressure axial turbine (2-stage) of an industrial turbomachine, where an actual turbine was used to collect experimental data and then compared with CFD results obtained from other studies (Pfau, 2003). Pfau (2003) utilized the following three seal types: an open inlet cavity, closed labyrinth cavity, and an open exit cavity. Subsequently, gap-to-blade height ratios of 0.3% and 0.8% were compared (Pfau, 2003). Since the tip clearance gaps were very small compared to blade height, Pfau (2003) developed a new probe measurement technology. Pfau (2003) was able to describe and quantify loss mechanism, develop theoretical models to analyze flow effects and provided recommendations and modifications to minimize tip losses.

CHAPTER 2

CFD METHODOLOGY

The study utilized CFD analysis to examine the tip clearance loss of 12 blade tip configurations. For each configuration, a CAD model was created and imported to the meshing software where a grid or mesh was generated. CFD software was utilized to run numerical solutions, where the same boundary conditions were applied to each configuration.

2.1 Procedure

During this study, the following three software were employed to complete the objectives: *(i)* CATIA for CAD, *(ii)* ICEMCFD for Meshing, *(iii)* and ANSYS-CFX for CFD software. When setting the meshing on several of the CAD models, a number of issues emerged that required re-editing of the CAD models. These problems were solved after two to four iterations. A similar scenario occurred when attempts were made to run the CFD simulation because of mesh issues; at some point, it was necessary to either re-create the mesh with different spacing grids or re-edit some of the CAD models. **Figure 2-1** shows the iteration process that was conducted during the study.
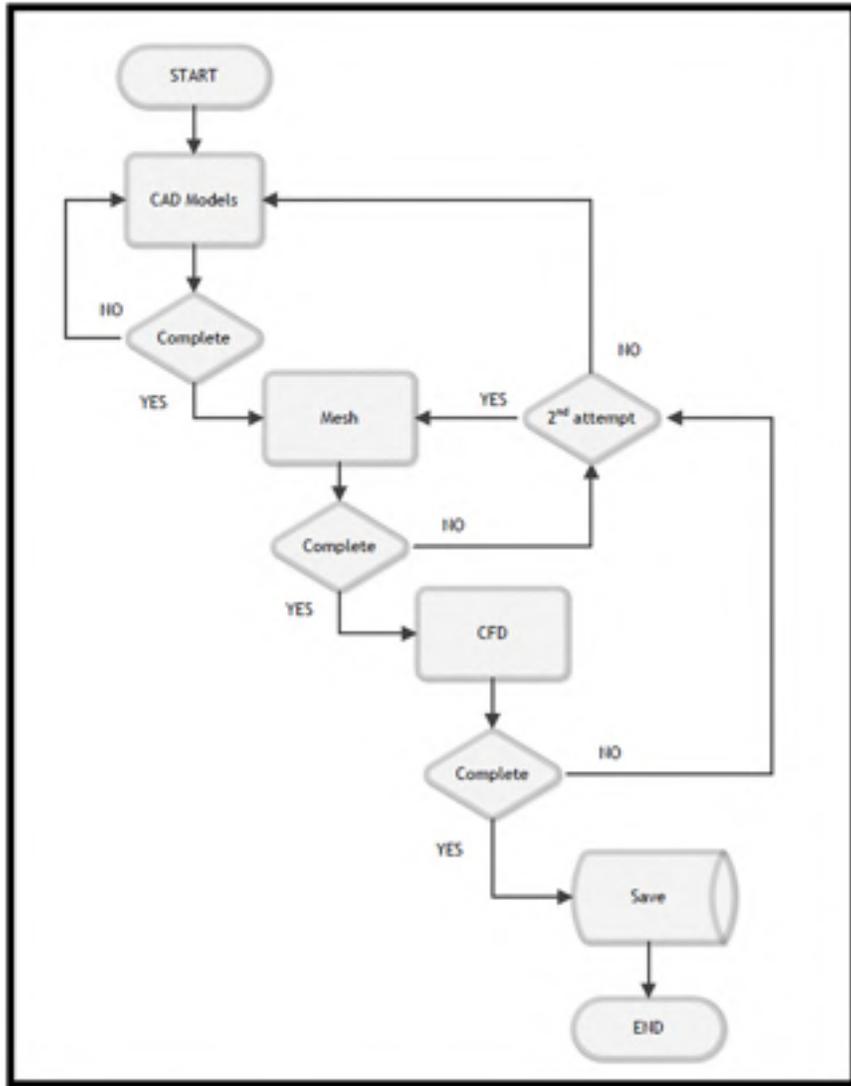
Figure 2-1 CAD, Mesh and CFD Models Iterations

2.2 Geometry

All configurations used the same blade but with different tip geometry designs. Each configuration was modeled using CATIA software with three different tip clearances of .015 in, .030 in and .048 in. Twelve different configurations, each of which had three different tip

clearances, and one configuration with zero clearance were modeled. Therefore, a total 37 CATIA models were created for the study.

2.2.1   Outer Wall Types

The casing wall or wall OD at the blade tip was also modified for each configuration. Shrouded blades with one, two, and three fins had two configurations each; one with straight casing wall and the other with stepped casing wall, as shown in **Figure 2-2**. The figure presents a one-stepped wall type of a shrouded two-fin blade configuration. In cases with a shrouded three-finned blade, the casing wall had two-steps.
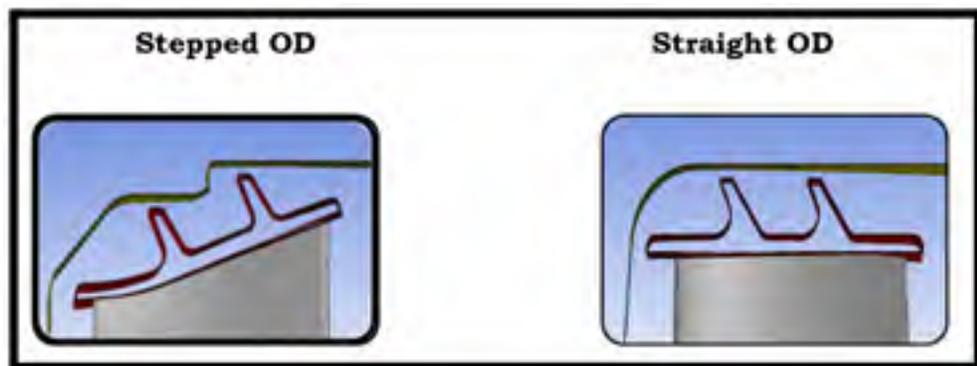
Figure 2-2 Wall Outer Diameter (OD) Types

2.2.2   Number Of Fins

The tip was modified to present the shrouded blade with one, two and three-fins as shown in **Figure 2-3** . When modifying the tip, the wall OD was adjusted in order to maintain the same clearance value.
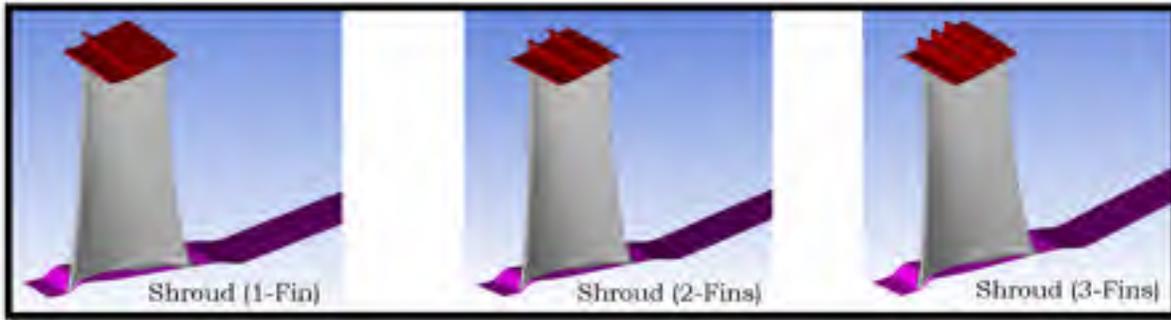
Figure 2-3 Blade Types

2.2.3   Fin Types

An experimental study by Stocker (1978) claimed that configurations with angled fins have less tip loss than vertical fins. Stocker (1978) presented the flow coefficient values of several stepped OD designs against the tip pressure ratio that showed an optimized angled fin seal with the lowest flow coefficient. Angled and vertical fins were included in this study to verify Stocker's claim, which indicated that angled fins have lower tip clearance loss than vertical ones. An example of a vertical and angled fin models used in the current study is presented in **Figure 2-4**.
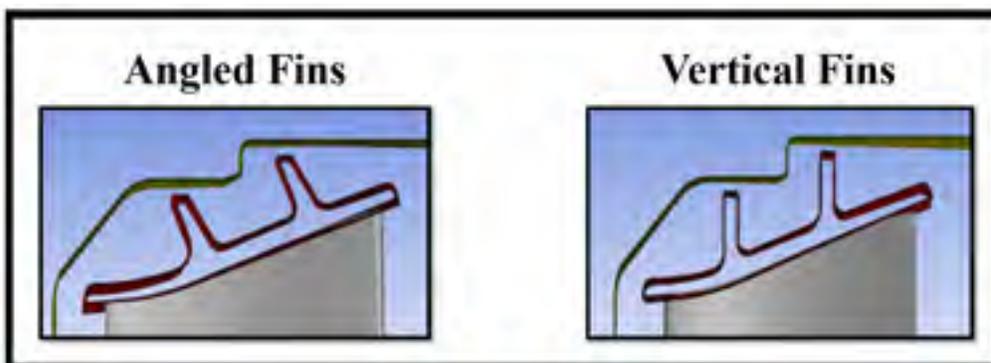
Figure 2-4 Fin Types

2.2.4   Configurations

After having defined blade tip, wall OD, and fin types, 12 configurations were created; they were divided into six-stepped OD and six straight OD. Both OD types included one, two and three angled and vertical fins. The 12 configurations were repeated to obtain three tip clearances of .015 in, .030 in and .048 in; therefore, 36 configurations were modeled plus one configuration with zero clearance, which was used as a reference. **Figure 2-5** shows the 12 configurations corresponding to .030-inch clearance.
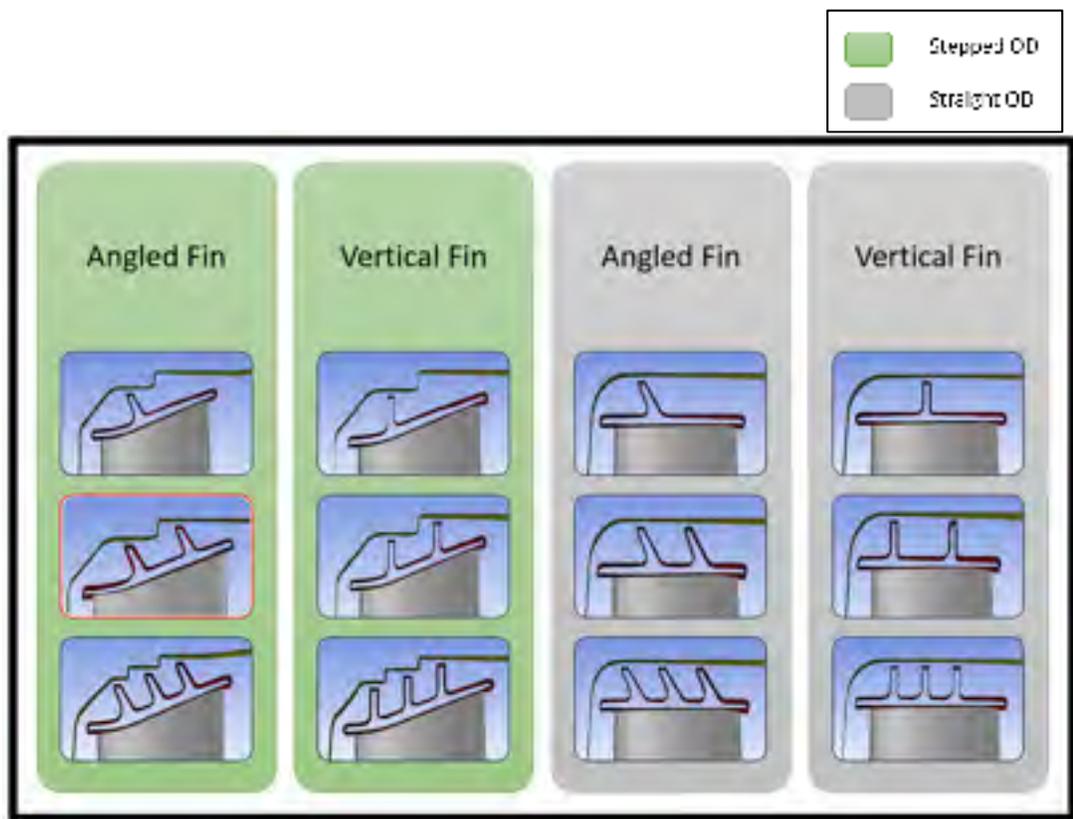
Figure 2-5 Shrouded Blade Configurations

Shrouded models maintained a constant clearance value since both the fin ends and casing wall are concentric. **Figure 2-6** displays the clearance that was modeled for all

configurations. The above-mentioned steps were followed when modeling the two and three finned configurations.
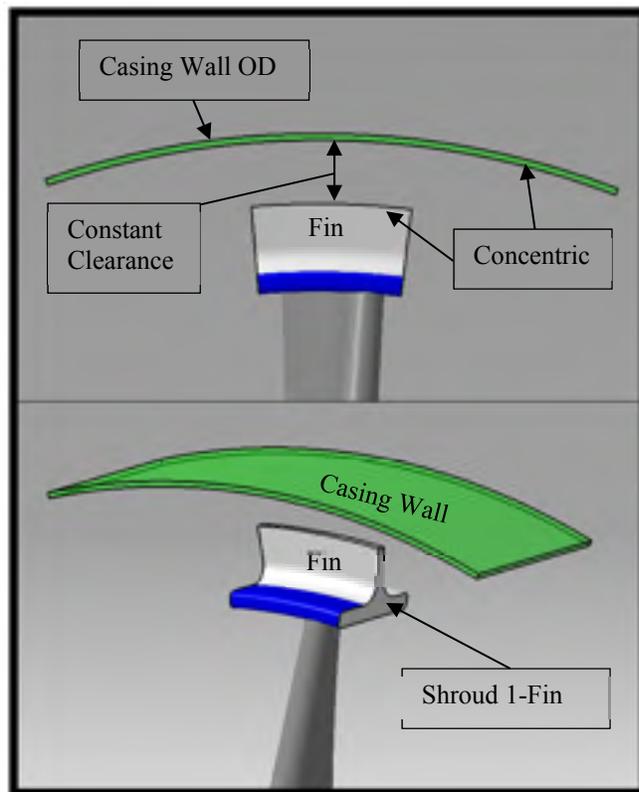
Figure 2-6 Tip Clearance

In addition, periodicities were kept identical by drawing one side then rotating it by an angle of approximately 10 degrees to create the second periodic plane. It was important to create them in the aforementioned fashion; otherwise, mesh models could not have been completed.

2.3   Mesh Sensitivity Study

Prior to meshing all configurations, a mesh study was carried out on one specific configuration to verify the mesh sensitivity and check its convergence of the total-to-total stage efficiency, which is defined in section 3.1.2. This step was performed on the shrouded, 2-fin and stepped OD configurations, where seven meshes were created, as is listed in **Table 2-1**. The first mesh shown in the first row of **Table 2-1** had the smallest mesh size, and the seventh mesh had the highest mesh size.

Once the seven mesh models were completed and their CFD solutions were obtained, their total-to-total stage efficiency (η_{tt}) values were evaluated using equation (3-1). Then the change in efficiency ($\Delta\eta$) with respect to mesh 1 was obtained for each mesh as shown in **Table 2-1**.

Table 2-1 Mesh Sensitivity

Mesh	# of Cells (N_{cells})	# of Nodes (N_{nodes})	$\sqrt[3]{N_{nodes}}$	$\Delta\eta$ w.r.t Mesh 1
1	48,251,108	15,356,965	249	0.00%
2	43,739,779	13,891,151	240	-0.02%
3	37,558,895	11,897,113	228	-0.03%
4	31,211,788	9,351,974	214	-0.08%
5	26,458,909	8,302,984	202	0.13%
6	19,926,374	6,181,380	184	-0.20%
7	15,731,527	4,827,919	169	-0.26%

The change in efficiency values were plotted against the cubic root of number of nodes, as is shown in **Figure 2-7**. The cubic root taken for the number of nodes represents the variation of the number of nodes in one-dimension. The last column corresponds to the change in the total-to-total stage efficiency with respect to mesh 1, which was completed in a span of 16 hours, whereas mesh 7 was prepared in one hour.
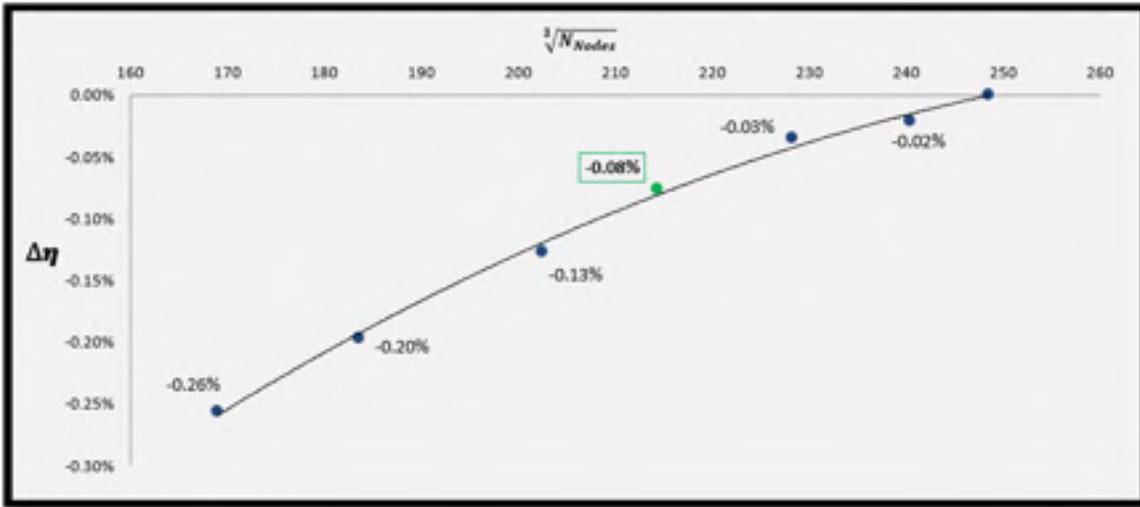
Figure 2-7 Mesh Study

As shown in **Figure 2-7**, mesh 4 ($\Delta\eta = -0.08\%$) was chosen for the analysis due the run time available to complete the project; mesh 4 was performed over 4 hours and included 9.8 million nodes. It was assumed that the difference between the results of the selected grid and the results of the converged grid would be the same for all configurations. Given that assumption, the difference in results between each configuration would have been due to change in tip geometry. It is also important to note that when increasing the number of fins at the blade tip area, the surface area is also increasing; and therefore, part of the losses could be related to friction or profile.

2.4   Mesh Generation Software

Once all configurations were modeled, they were imported into commercial meshing software (ICEM CFD) to create an unstructured mesh that consists of tetrahedral elements and prisms to refine the boundary layer. Surface mesh was initially generated with a size of .030 inches; it was manually reduced to .003 inches to resolve the flow physics in the tip clearance region. A fine mesh sizes were picked on the leading edge, trailing edge, all fillets,

and at the tip and shroud areas. In addition, a fine mesh was selected, and other boundaries has relatively larger mesh size as specified in **Table 2-2**.

Table 2-2 Surface Mesh Sizes

Boundary	Mesh size (TRI) [inches]
Fin tip Mesh Density	.003
Leading Edge, Trailing Edge, Blade Fillets, and Shroud	.005
Shroud Mesh Density	.010
Inner Diameter, Outer Diameter, Stage Inlet, Stage Outlet, Blade Suction Side, Blade Pressure Side, and Periodicities	.040

Prisms were created at all walls with a height limit factor of 2.5 and with a growth ratio of 1.5. These prisms contained 15 layers with initial total height (h_t) value set to .044 inches. All y^+ parameter values were one or less. Prism height limit factor is the ratio between h_t and the maximum mesh size (e_{max}) defined in **Figure 2-8**. This allows smooth transition from prism to TETRA elements, for the capturing of the turbulent boundary layer effects at all walls. Since the focus of this study was to investigate blade tip leakage, a fine mesh was chosen at the tip area (shroud plus fins) as outlined through **Figure 2-9** to **Figure 2-11**. Small edges, such as leading edge and fillets, were assigned a very fine grid relative to other surfaces.
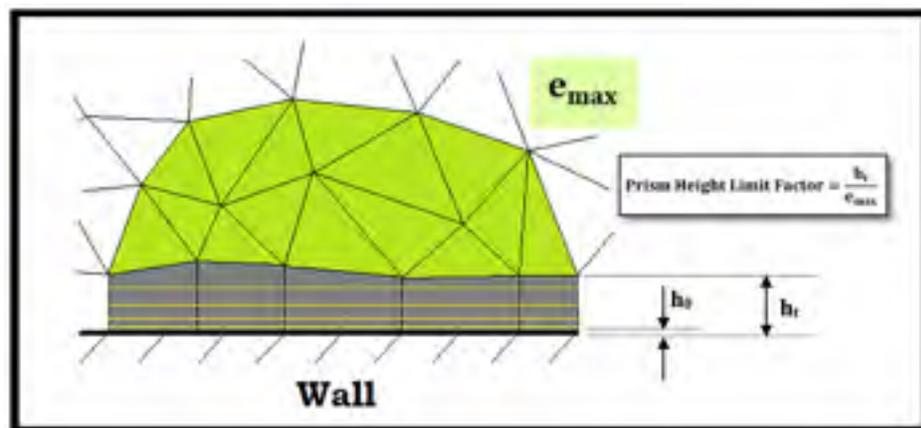
Figure 2-8 Prism Height Limit Factor

Figure 2-9 Fine Density Grid at Tip Clearance
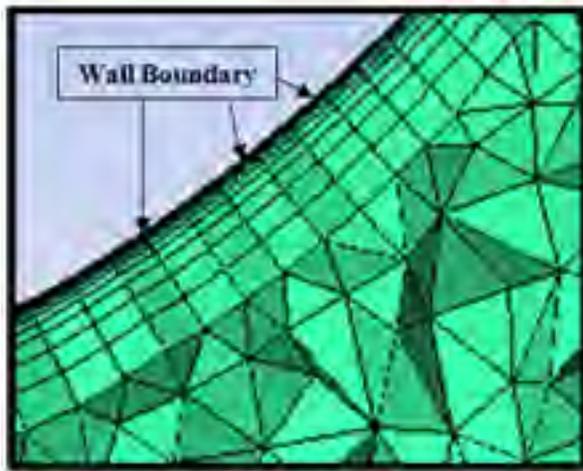
Figure 2-10 Wall Grid Sections

Figure 2-11 Trailing Edge Grid

2.5   Boundary Conditions

Circumferentially averaged radial profiles of total pressure "P_t", total temperature "T_t", and flow inlet angle "α", with turbulence quantities (5% turbulence intensity) of turbine kinetic energy and turbine dissipation rate, were set at the vane inlet. Circumferentially averaged radial profiles of static pressure "P_s" were set at the blade exit. Wall boundaries were set to adiabatic and no-slip conditions. Rotational periodicities were chosen normal to the inlet and exit plans.

The mixing plane concept was introduced since the stage model contained a stationary component (Vane) and a moving component (Blade) as shown in **Figure 2-12**. Swirl conservation option was used, which transfers momentum between the vane exit and the blade inlet (at mixing plane interface). This was able to determine the tangential velocity component to the full mixing plane area (360 degrees) and then adjust the profile such that the momentum is equal on both sides of the domains (fixed and rotating) (ANSYS Modeling Guide, 2013).
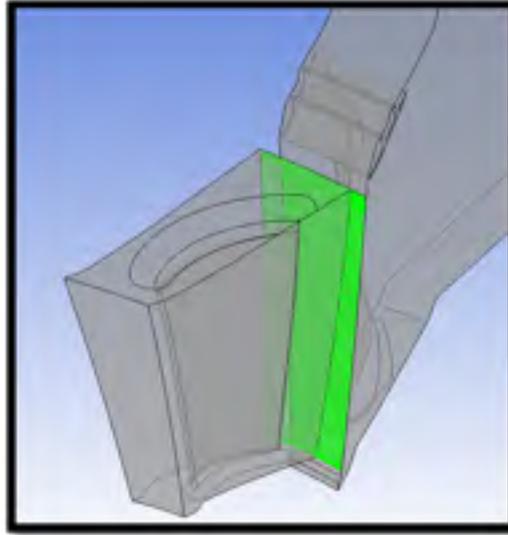
Figure 2-12 Mixed Plane

2.6   Computation Fluid Dynamics Analysis

Once successfully completed, meshed models were imported into a commercial simulation software (ANSYS-CFX). Identical boundary conditions were utilized for all configurations. As shown in **Figure 2-13**, vane and blade domains were completed separately and both domains were imported into the CFD software as an assembly. The same vane domain and mesh was used on all configurations. Once a simulation was completed (2-angled fin with straight OD), another blade domain was replaced (2-angled fin with stepped OD) and so on until CFD results were obtained for all configurations.
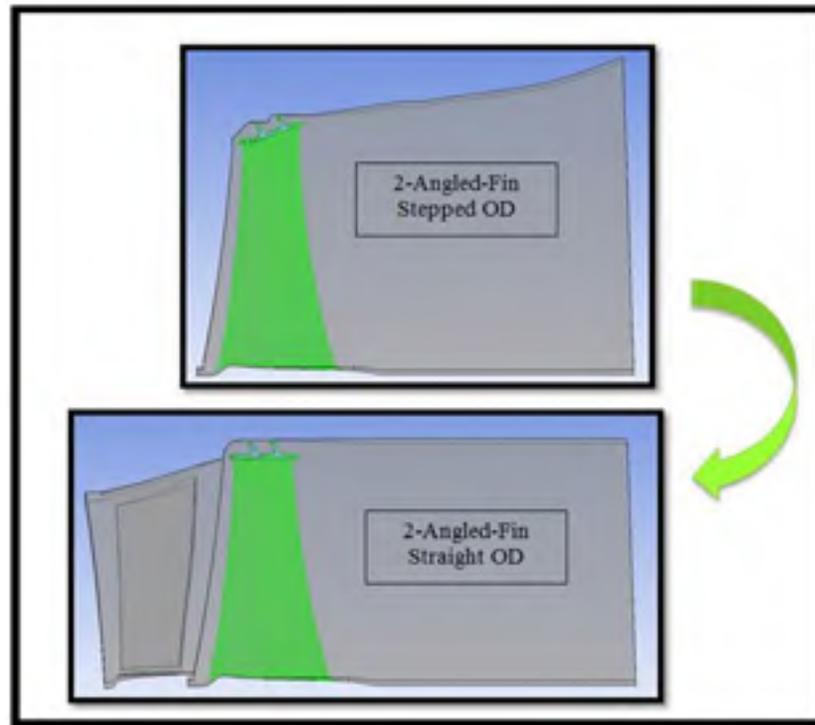
Figure 2-13 Vane and Blade Domains

The K−ω Shear Stress Transport (SST) turbulence model was employed. It is a combination of K−ε and K−ω equation models, where it utilizes the former model to solve properties in the bulk flow and the latter near the walls. Moreover, it includes a blending function to ensure a smooth transition between the K−ε and K−ω models. Previous studies showed that the SST model is an effective, robust and reliable tool for turbomachinery applications (Mangani, Casartelli, Wild, & Spyrou, 2014), (Hanimann, Mangani, Casartelli, Monkulys, & Mauri, 2014) and (Wang, 2014).

In this study, air was selected as the working gas with steady Reynolds-Averaged Navier-Stokes (RANS) equations as the selected methodology, CFX standard second-order artificial dissipation model, and fully turbulent flow. No additional modeling such as combustion, radiation, etc., was selected.

2.7 Summary

There were three softwares used during this study: *(i)* CATIA for CAD, *(ii)* ICEMCFD for Meshing, and *(iii)* ANSYS-CFX for CFD. A configuration is defined as a combination of the following: *(i)* outer diameter type (straight vs. stepped), *(ii)* number of fins (up to three fins) and *(iii)* fin type (vertical vs. angled). Each configuration has three-tip clearance values (.015, .030 and .048 inches) and only one model was created to have no clearance to locate total-to-total efficiency value with zero-inch clearance value. Therefore, 37 configurations were created for this study. A mesh sensitivity study was performed on one model to create an unstructured mesh with its sizes chosen according to available computing resources, and available run time to complete this study. Same boundary conditions were set for each configuration; circumferentially averaged radial profiles (total pressure, total temperature, and flow inlet angle) with 5% turbulence intensity of turbulence kinetic energy and dissipation rate were set at the vane inlet. In addition, circumferentially averaged radial profile (static pressure) was set at the blade exit. Wall boundaries were set to adiabatic and no-slip conditions and rotational periodicities were chosen normal to the inlet and exit plans. The mixed plane concept was implemented to simulate the transition between fixed (Vane) and rotating (Blade) domains. This concept is recommended by ANSYS when simulating two zones: stationary zone (Vane) and rotating zone (Blade) where data are averaged in the circumferential direction between vane exit and blade inlet. The SST turbulent model was utilized.

CHAPTER 3

RESULTS AND ANALYSIS

3.1 Stepped OD vs. Straight OD Configurations

This section outlines the comparison of CFD results for all configurations. These comparisons were made by plotting the following: *(i)* change in total-to-total stage efficiency against clearance-to-span ratios; *(ii)* mass flow at blade tip area against number of fins; *(iii)* total-to-total stage efficiency against mass flow at blade tip area; and tip clearance, *(iv)* and velocity streamlines.

The configuration with zero clearance was modeled and then used to run CFD simulation to acquire a reference value for total-to-total stage efficiency, which was used to determine the location on the efficiency axis (y-axis). This particular efficiency value was subtracted from the efficiency values of all other configurations; these values were subsequently plotted in a graph against tip clearance to span ratios as shown in **Figure 3-5** and **Figure 3-6**.

3.1.1 Convergence

Figure 3-1 is an example of a convergence plot for one case, where it shows solution imbalances of variable values (y-axis) against number of iterations (x-axis). Convergence criteria were set to 10^{-8} of RMS, and the number of iterations required for flow convergence was set to 500 iterations. As shown through **Figure 3-1** to **Figure 3-3**, values converged between 10^{-4} and 10^{-6} of RMS for the 2-angled fin with stepped OD configuration.
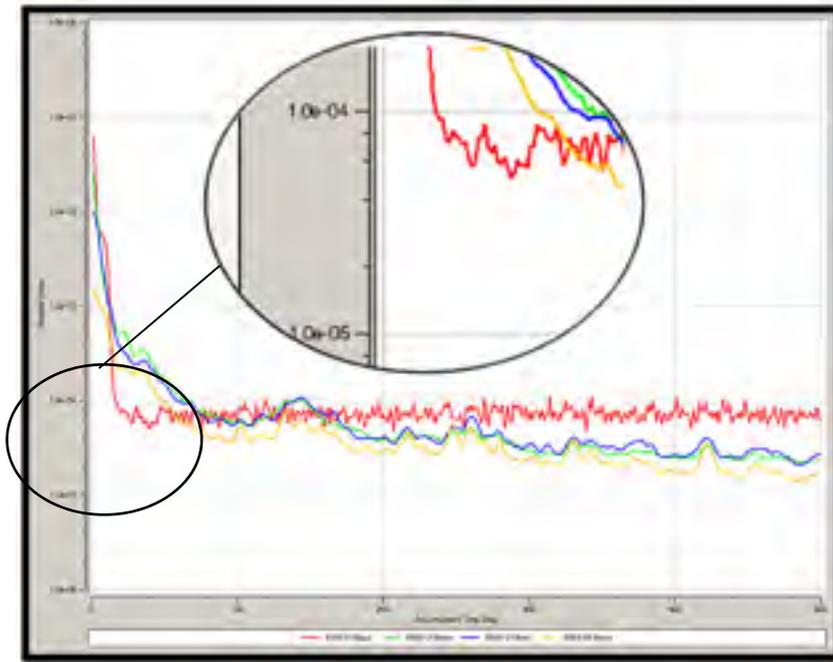
Figure 3-1 Momentum Convergence
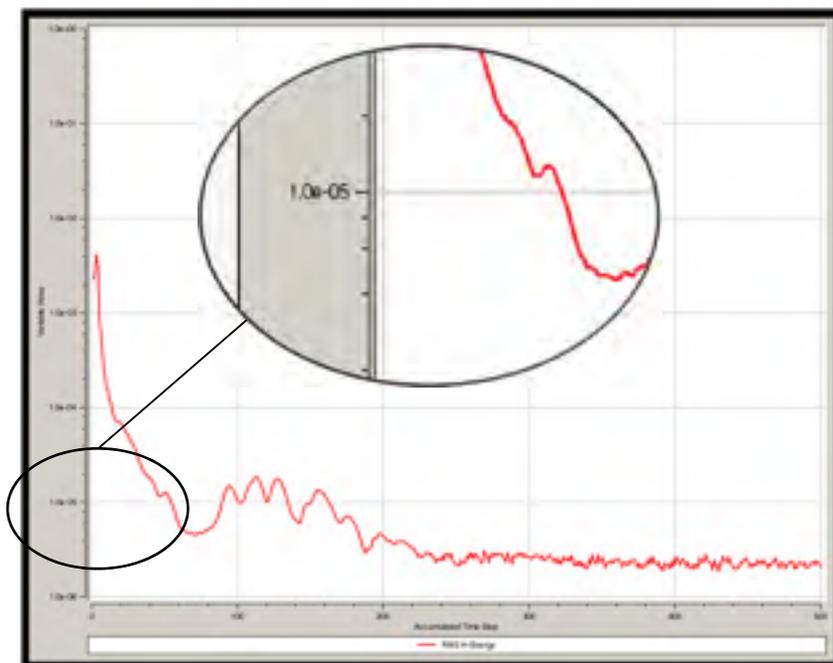
Figure 3-2 Energy Convergence
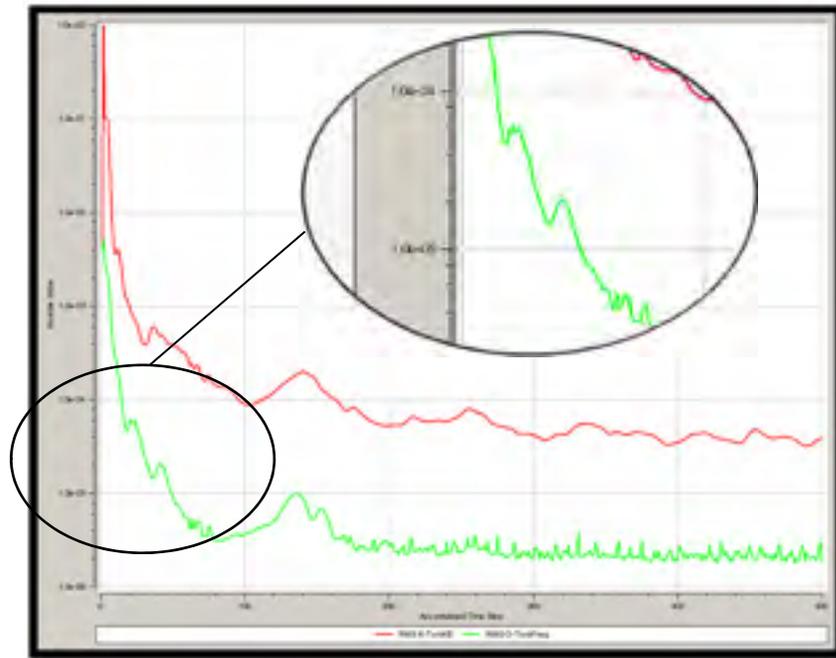
Figure 3-3 Turbulence Convergence
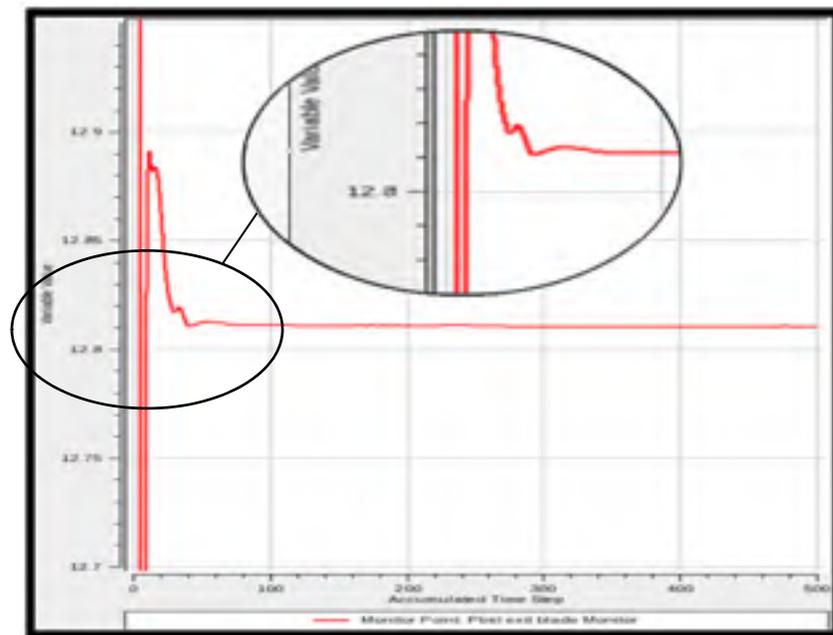
Figure 3-4 Flow Property (Relative Pressure) Convergence

Figure 3-4 is an example of the relative pressure convergence, where one flow property was randomly selected. The relative pressure variable at blade exit converged after 50 iterations to 12.81 psi as indicated in the figure below.

3.1.2   CFD – Calculated Efficiency

The total-to-total stage efficiency values for all configurations were evaluated using **equation (3-1)**. Given the stage inlet temperature $(T_{t,in})$, stage pressure ratio (P_r), and average gas ratio of specific heats (γ), the isentropic temperature at stage exit $(T_{ex,isen})$ was evaluated using **equation (3-2)**. With temperature and pressure known, enthalpies at inlet and exit were obtained from the gas tables (Cengel, 2007) and ideal Δh was evaluated using **equation (3-3)**, which was also used to evaluate the actual Δh from data obtained from CFD.

$$\eta_{tt} = \frac{\Delta h_{Actual}}{\Delta h_{Ideal}} \tag{3-1}$$

$$T_{isen,ex} = T_{t,in} \times \left[\frac{1}{P_r^{\left(\gamma-1/\gamma\right)}} \right] \tag{3-2}$$

$$\Delta h = h_{in}\_h_{ex} \tag{3-3}$$

Figure 3-5 and **Figure 3-6** present the change in total-to-total stage efficiency with respect to efficiency with zero clearance, versus the clearance-to-span ratios for angled and vertical fins respectively. All stepped OD configurations were found to have greater efficiency, at the same tip clearance to span ratio, than all straight OD. CFD results also revealed that a greater number of fins corresponded to increases in efficiency for both stepped and straight OD configurations. This was expected because the addition of fins to the shroud increases flow resistance at the tip and thus results in decreasing the mass flow at the blade tip area.
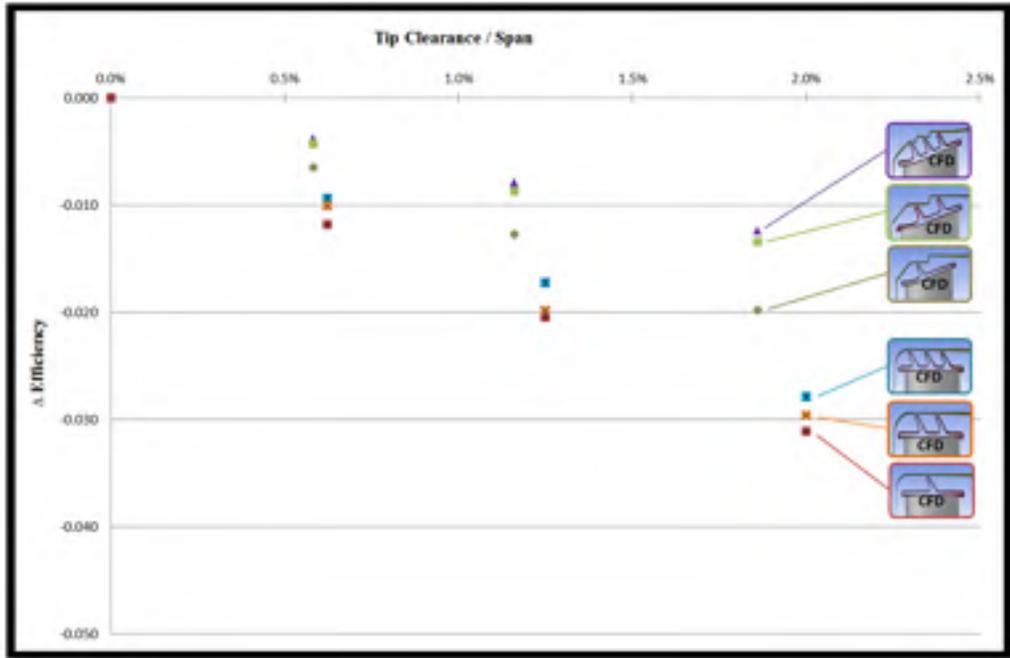
Figure 3-5 CFD - Change in total-to-total Stage Efficiency for Angled Fins
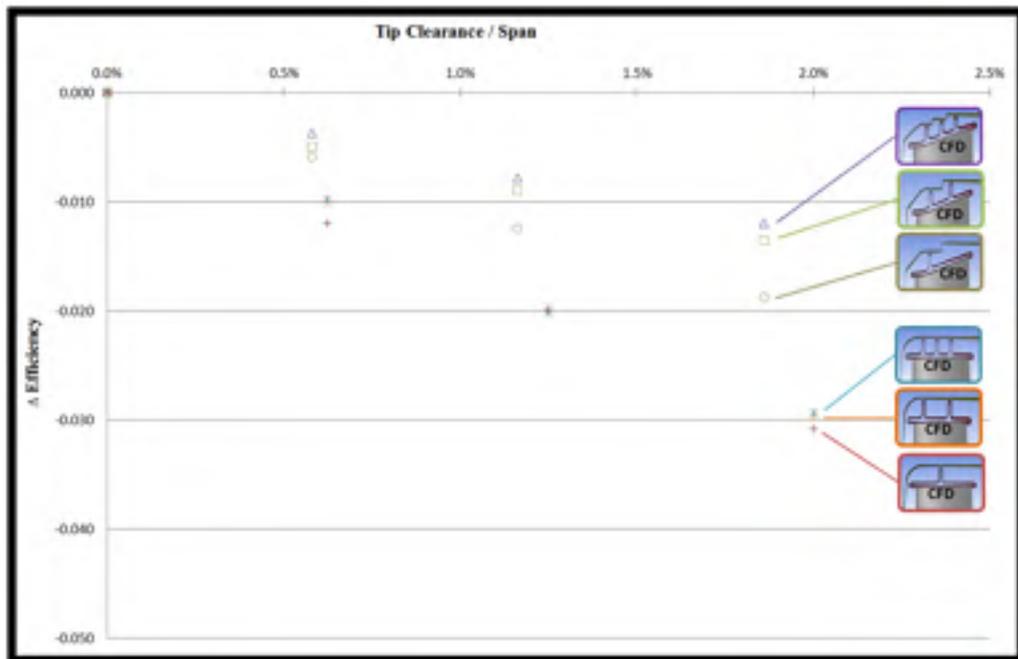
Figure 3-6 CFD - Change in total-to-total Stage Efficiency for Vertical Fins

Furthermore, small differences were found when comparing efficiency values for angled and vertical fin configurations. Angled fins did not always show greater efficiency than vertical fins. This inconsistency was observed for the remainder of the configurations as shown in **Figure 3-5** and **Figure 3-6**. The difference in efficiencies for configurations with two and three fins, as shown in **Figure 3-5** and **Figure 3-6**, was less than that found between configurations with one and two fins.

3.1.3   CFD – Mass Flow

Mass flow values at blade tip area were retrieved by creating two planes at each of the tip inlets and exits for stepped (left) and straight (right) OD configurations, as presented in **Figure 3-7**. Mass flow values of all configurations were plotted against number of fins and tip clearances to compare flow tip leakage.
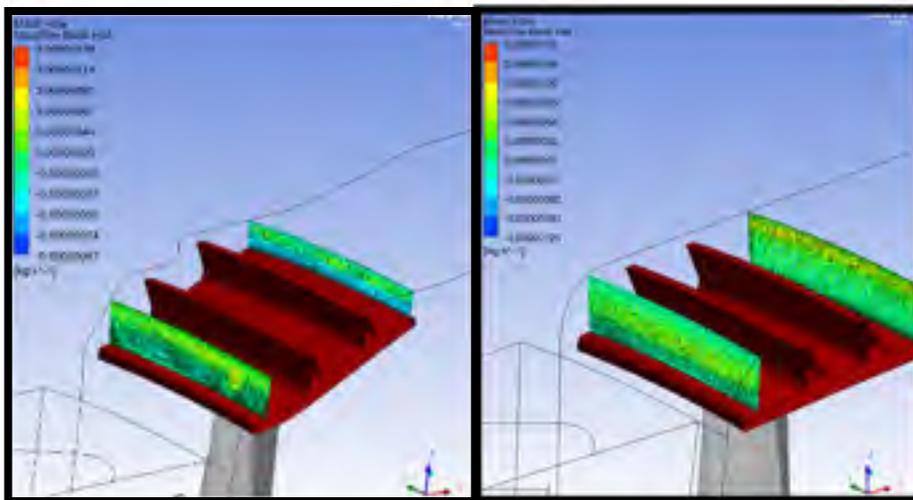
Figure 3-7 Inlet and Exit Planes at Shroud Tip (Stepped and Straight)

When plotting the tip mass flow against the number of fins for all configurations with multiple tip clearances, stepped OD configurations had lower tip mass flow than straight OD. **Figure 3-9** shows the tip mass flow for angled fins, which includes the three different

clearances for stepped OD (hatched lines) and straight OD (solid lines) configurations. In addition, each plot has an inclined slope, which causes tip leakage to decrease as the number of fins increase. Tip mass flow values exhibited consistency in terms of clearance values for both stepped and straight OD; the smaller the tip clearance, the lower the mass flow.
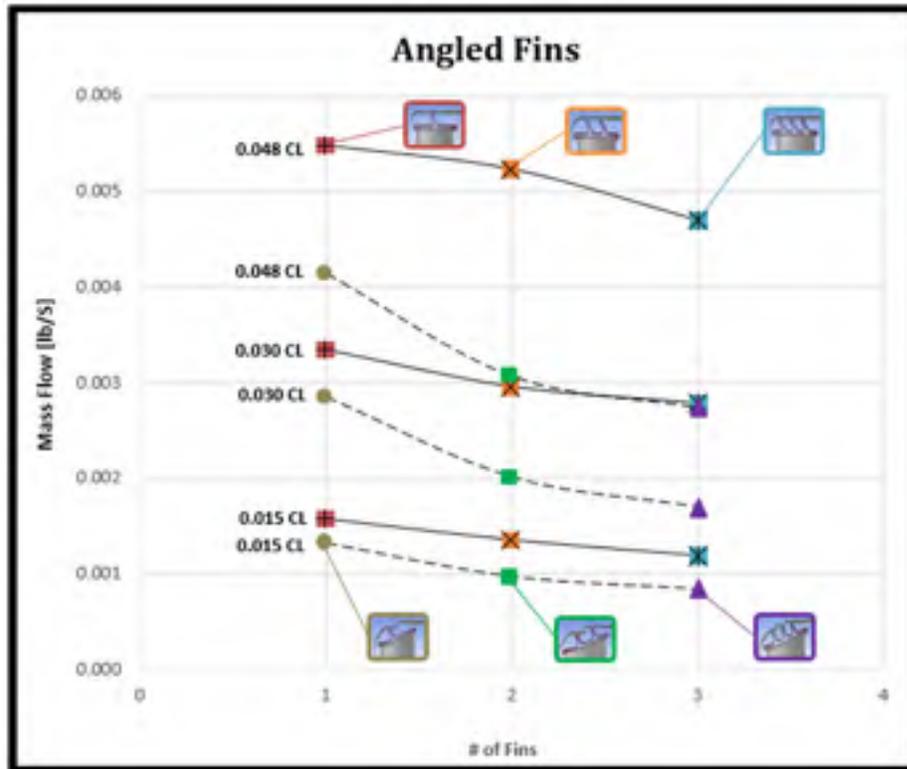
Figure 3-8 Mass Flow vs. Number of Fins – Angled

A comparable plot was created for vertical fins, which exhibited very similar results to angled fins, and is shown in **Figure 3-9**. The 3-vertical fin with straight OD configuration with .030 and .048 inch clearances did not show a lower mass flow than 2-vertical fin with straight OD configuration. When comparing these to the corresponding angled fin with straight OD configurations, the angled fin had lower mass flow.
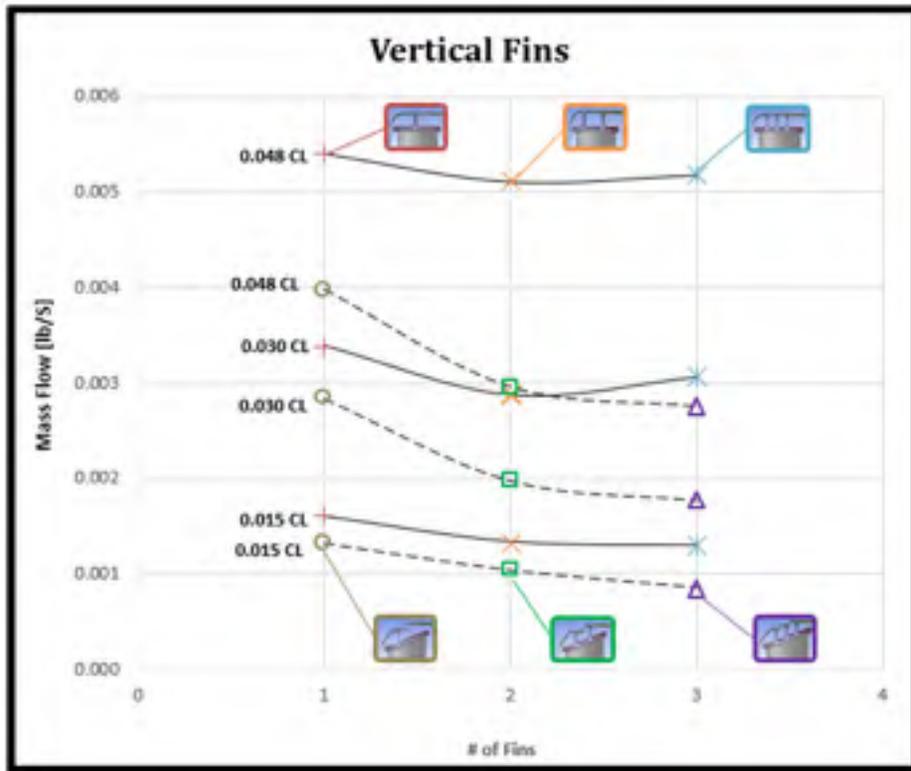
Figure 3-9 Mass Flow vs. Number of Fins - Vertical

3.1.4 CFD – Streamlines

Velocity streamlines retrieved from CFD simulation captured the flow over tip area for all configurations and are presented from **Figure 3-11** to **Figure 3-16**. The CFD legend of all streamline figures can be found in **Figure 3-10**. Each figure contains three rows and two columns. The first, second and third rows correspond to three different tip clearances of .0150, .0301 and .0482 inches respectively. The first and second columns correspond to configurations with angled and vertical fins respectively. When present, the arrow in the figure identifies flow disturbance downstream from the tip area. **Figure 3-11** presents velocity streamlines for stepped OD configurations of 1-fin with angled and vertical fins, which are located in the first and second column respectively.   As the tip clearance

increases, streamline shows flow separation downstream from the shroud. Angled and vertical configurations presented nearly identical streamlines.
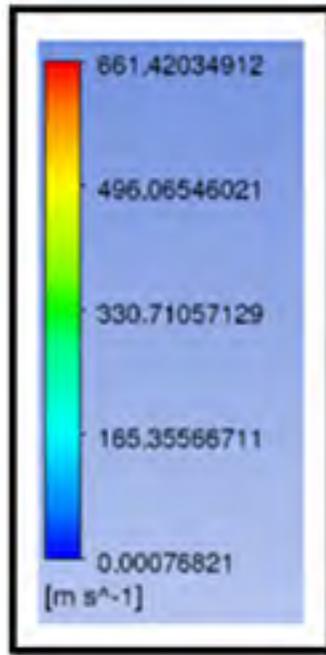
Figure 3-10 CFD Legend
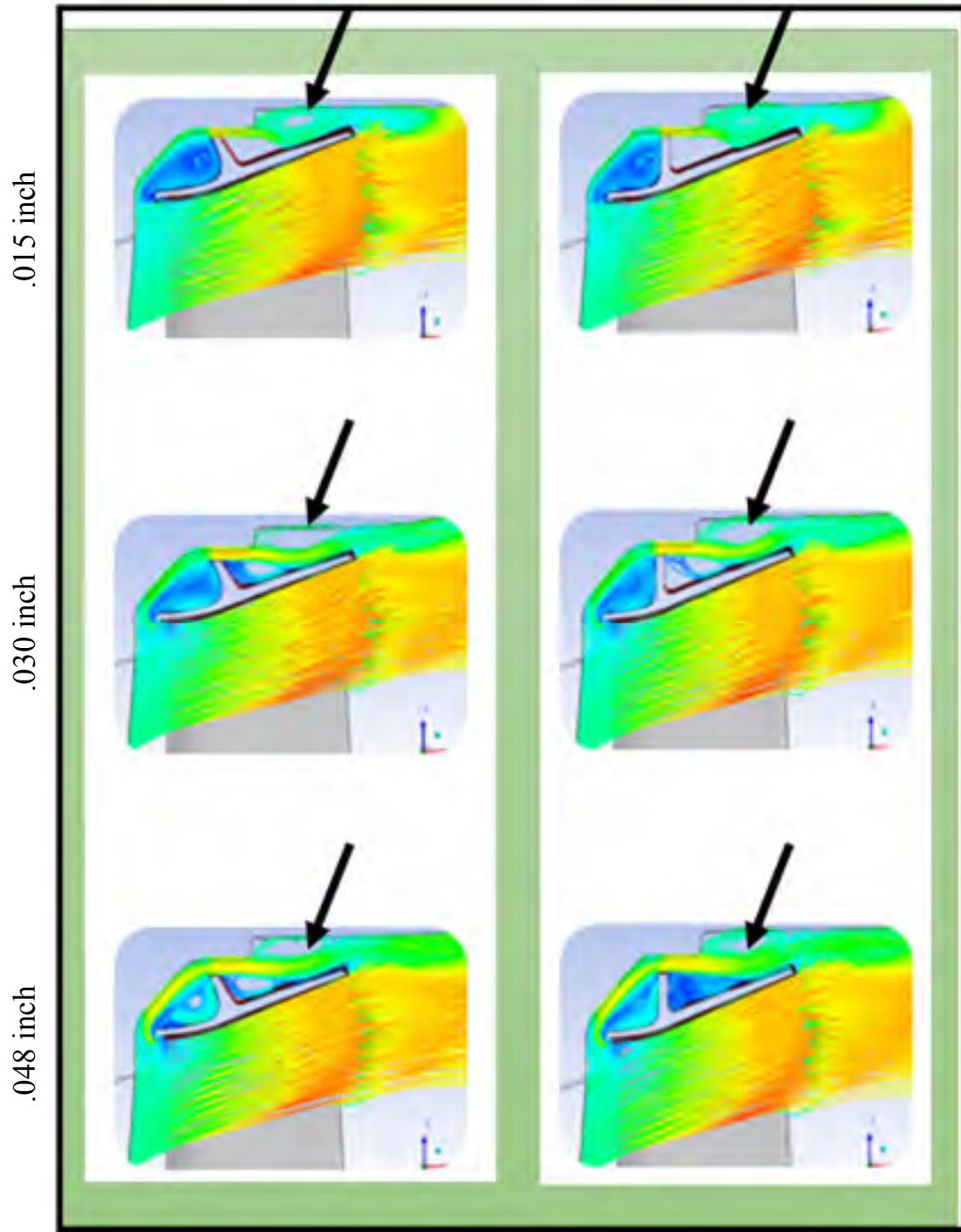
Figure 3-11 Velocity Streamlines for Stepped OD with 1-Fin (Angled vs. Vertical)
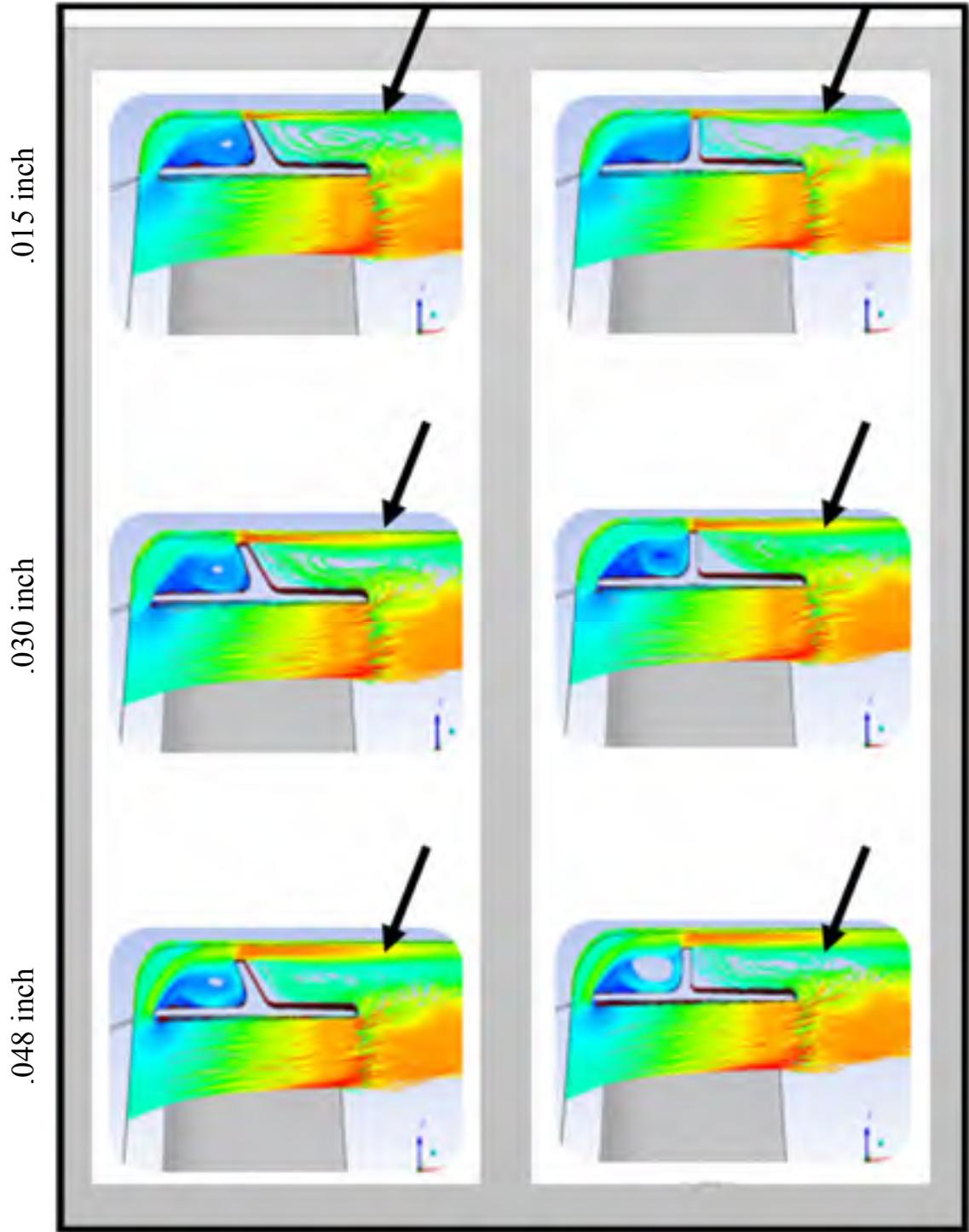
Figure 3-12 Velocity Streamlines for Straight OD with 1-Fin (Angled vs. Vertical)

Figure 3-12 shows streamlines for straight OD configurations for 1-fin with angled and vertical fins, which are located in the first and second column respectively. When compared to **Figure 3-11**, streamline disturbance is prominent in straight OD configurations for any tip clearance. Angled and vertical fins show very similar patterns.

Figure 3-13 presents velocity streamlines for stepped OD configurations for 2-fins with angled and vertical fins, which are located in the first and second column respectively. Streamlines appear more condensed than the configurations with 1-fin; this is because the second fin acts as an additional resistor to the flow at the tip area. The vertical fin configuration with the highest tip clearance (bottom right of **Figure 3-13**), shows some separation in the streamlines downstream from the tip flow. This is not the case for the angled fin of the same clearance. When comparing 2-fins (**Figure 3-13**) to 1-fin (**Figure 3-11**) stepped OD configurations for all tip clearances, 2-fins exhibited more guided streamlines than 1-fin. This is due to the addition of an extra fin, which created more resistance at the tip and hence acted as a better seal. Once again, when comparing angled and vertical fins in **Figure 3-13** very similar streamline behavior was identified except in cases with vertical fins and high tip clearance.

Figure 3-14 shows the streamlines of straight OD configurations for 2-fins with angled and vertical fins, which are identified in the first and second column respectively. When compared to stepped OD configurations (**Figure 3-13**), streamline disruptions are more noticeable in straight OD configurations, as indicated by the arrow in **Figure 3-14**. Stepped OD with 2-fins configurations showed smoother flow at tip area than straight OD with 1-fin and 2-fins.
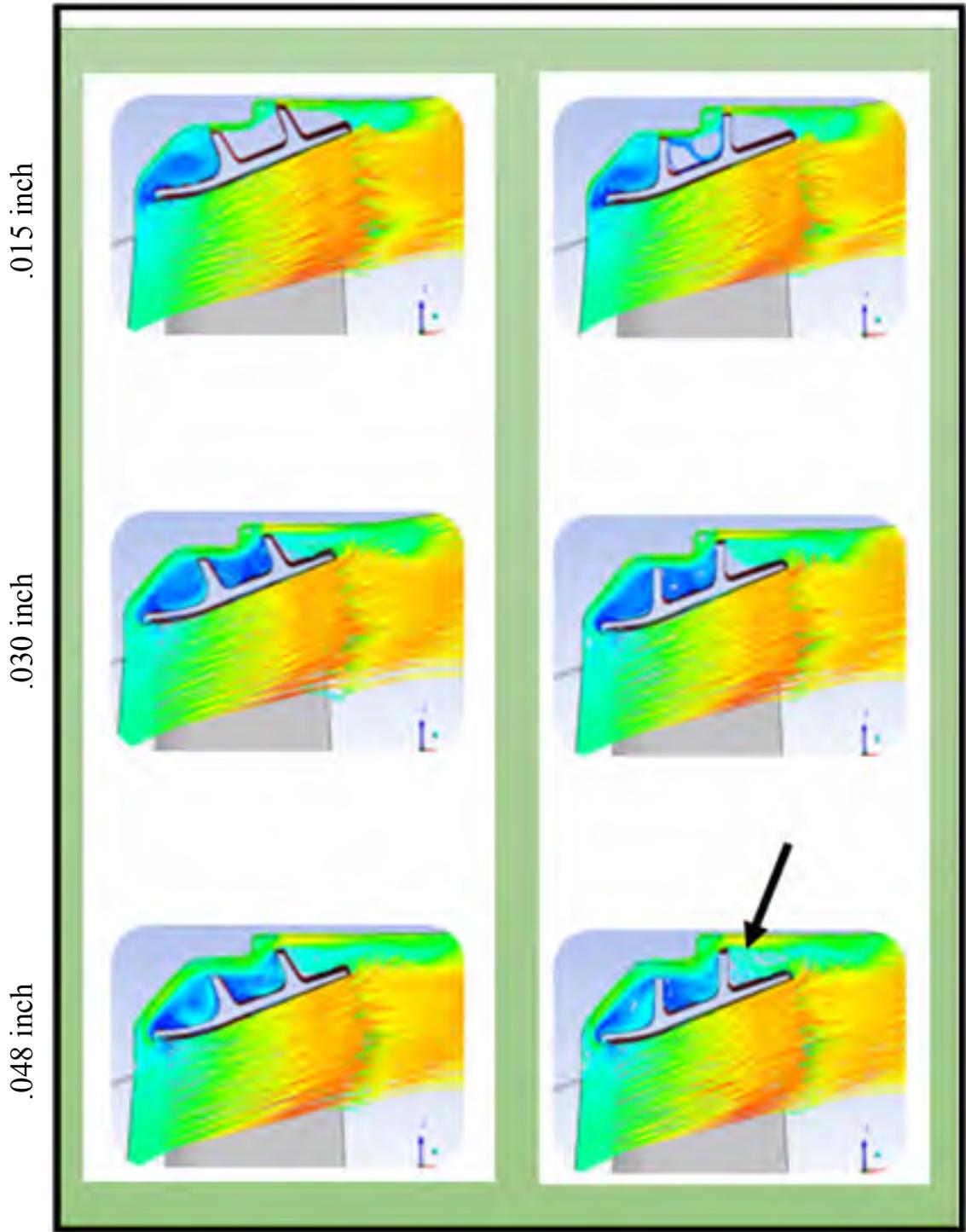
Figure 3-13 Velocity Streamlines for Straight OD with 2-Fins (Angled vs. Vertical)
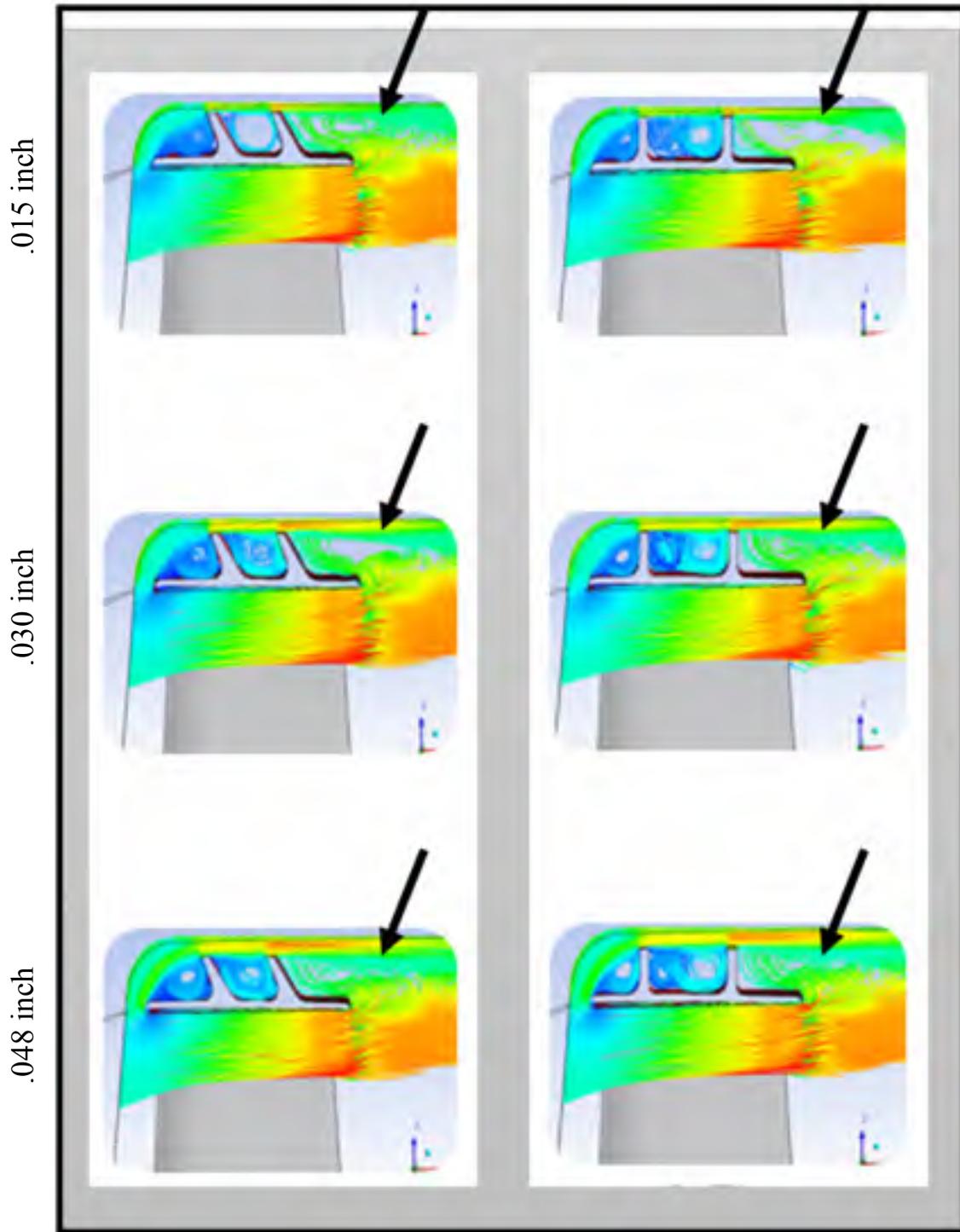
Figure 3-14 Velocity Streamlines for Straight OD with 2-Fins (Angled vs. Vertical)

Figure 3-15 displays velocity streamlines of stepped OD configurations for 3-fins with angled and vertical fins, which are represented in the first and second column respectively. Stepped OD configurations revealed glossier velocity streamlines than the 1-fin and 2-fins configurations; however, were found to be very similar to the 2-fins configurations. The addition of fins acted as a barrier to flow at the tip area and in the case of a stepped OD wall, streamlines at the tip area appeared to show better flow when compared to straight OD configurations.

Figure 3-16 displays velocity streamlines of straight OD configurations for 3-fins with angled and vertical fins, which are located in the first and second column respectively. Once again, straight OD configurations showed flow disturbance downstream from the tip area.

48
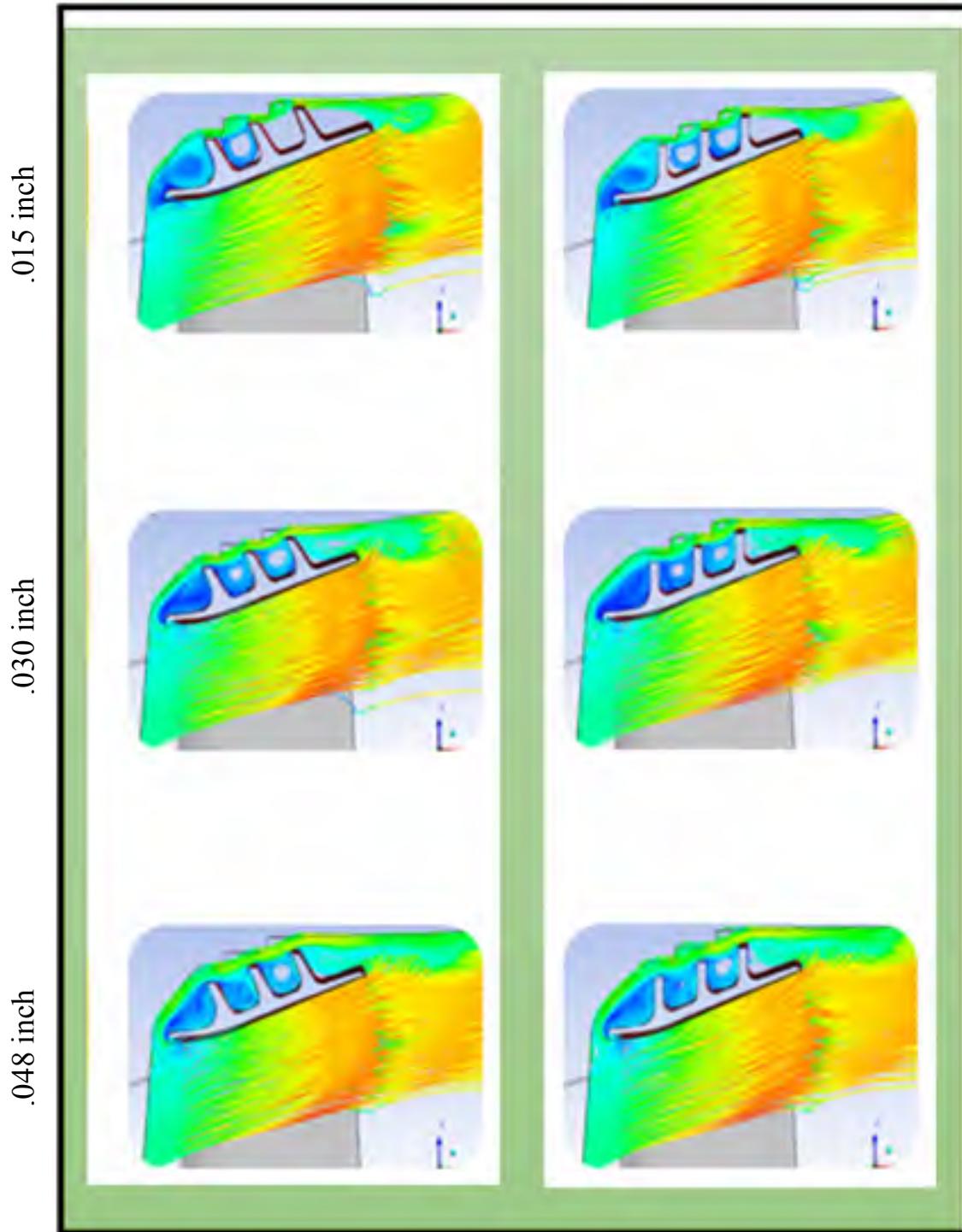
Figure 3-15 Velocity Streamlines for Stepped OD with 3-Fins (Angled vs. Vertical)
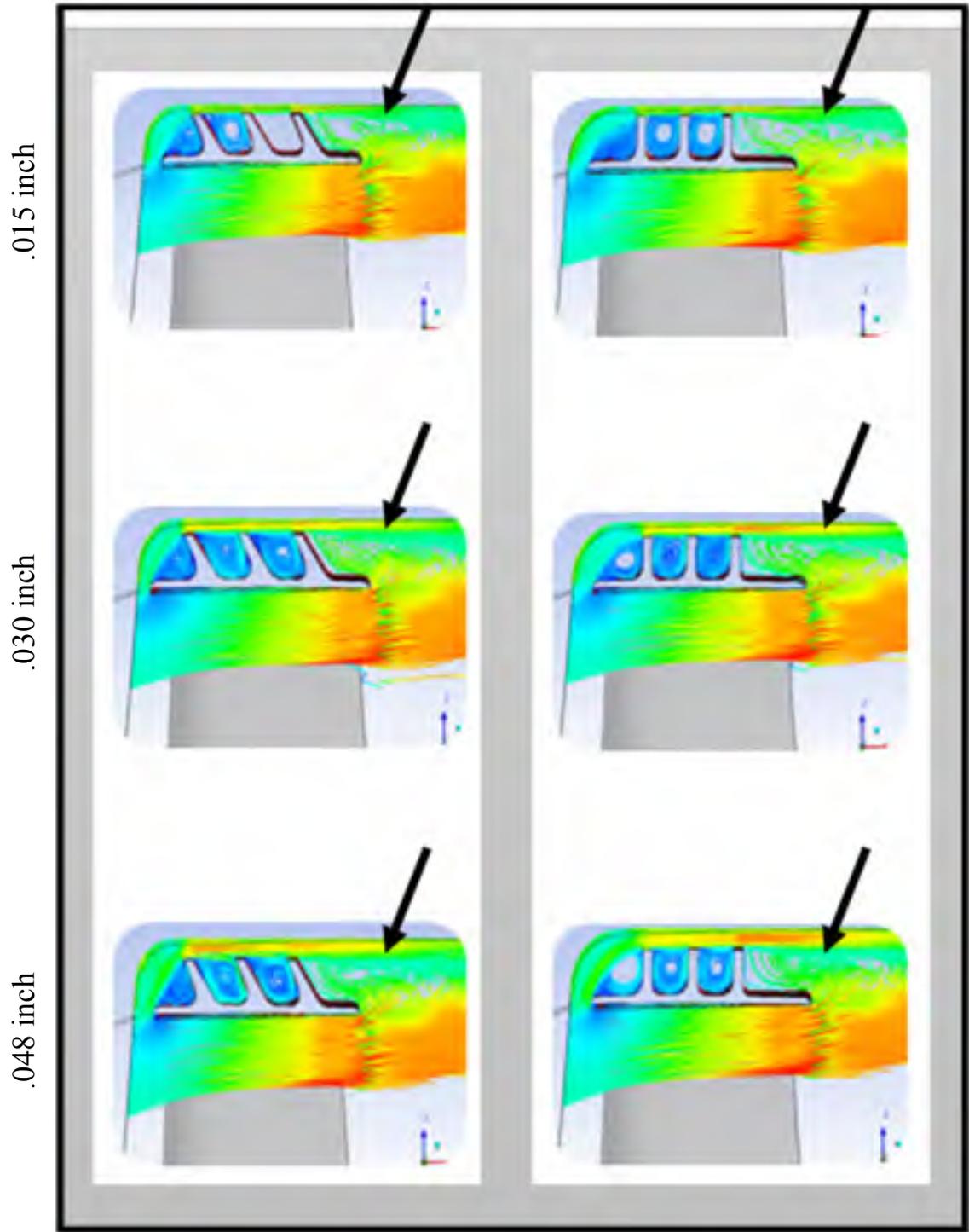
Figure 3-16 Velocity Streamlines for Straight OD with 3-Fins (Angled vs. Vertical)

Flow disturbance was evident when looking at the streamlines for straight OD configurations for 1-, 2- and 3-fins, as shown throughout **Figure 3-11** to **Figure 3-16**. This behavior contributed to the overall stage losses and eventually to total-to-total stage efficiency when compared to the stepped OD configurations, as is shown in **Figure 3-5** and **Figure 3-6**. For any number of fins, mass flow values, which are shown in **Figure 3-9**, and efficiency values, shown in **Figure 3-5** and **Figure 3-6,** exhibit the direct effect of tip mass flow on efficiency.
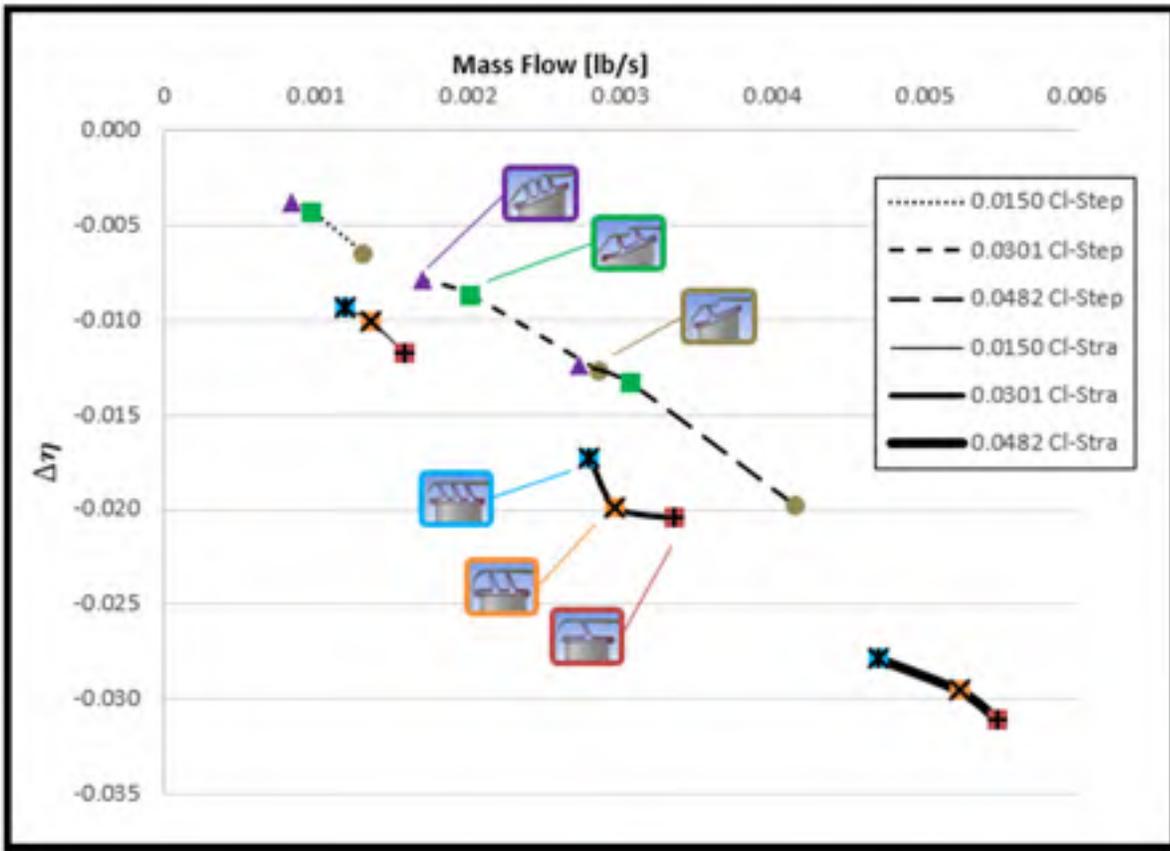
Figure 3-17 Change in Efficiency vs. Mass Flow for Stepped and Straight OD (Angled Fins)

When plotting the change in efficiency (section **3.1.2**) against mass flow values (section 3.1.3) for all configurations, **Figure 3-17** and **Figure 3-18** reveal that all stepped OD configurations (hatched lines) show higher efficiency than straight OD configurations. In addition, the smallest tip clearance values for stepped OD marked higher efficiencies for stepped and straight OD configurations. Moreover, consistency was identified for stepped OD configurations for both angled and vertical fins, where the change in efficiency increased as the mass flow decreased.
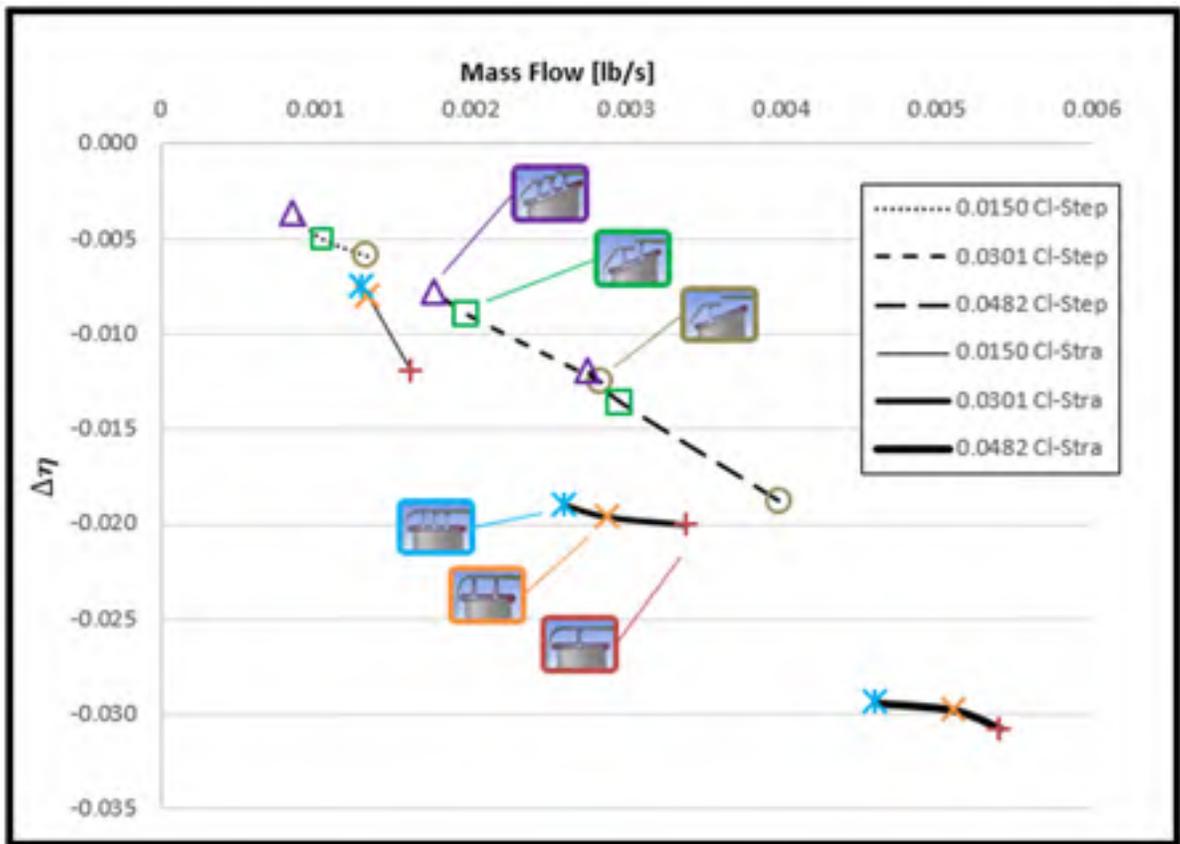
Figure 3-18 Change in Efficiency vs. Mass Flow for Stepped and Straight OD (Vertical Fins)

On the other hand, straight OD configurations for both angled and vertical fins exhibited varying trends where a big gap was identified between curves of different tip clearance values. Each curve demonstrated an increasing change in efficiency as the mass flow decreased but with a different slope.

3.2 Updated Tip Loss Correlation (Kacker & Okapuu, 1982)

This section discusses the modifcations made to Kacker & Okapuu's (1982) tip loss correlation (experimental-based); the equation is presented in **equation (1-2)**. Initially, total-to-total stage efficiencies for all configurations were evaluated by running the mean-line tool using the tip clearance loss correlation presented by Kacker & Okapuu (1982). These experimental efficiencies were then compared to efficiencies determined from CFD analysis. Afterwards, experimental tip loss correlations [**equation (1-2)**] were modified until experimental total-to-total stage efficiency values were aligned with CFD values.

The modifications were carried out on Kacker & Okapuu's (1982) tip loss correlation for every configuration. Updated correlations were concluded by evaluating different constants ranging from 0.10 to 0.50, along with their corresponding stage efficiency values. Subsequently, the Root Mean Square Error (RMSE) technique was utilized to calculate minimum error between efficiency values (this corresponded to the five constants) and CFD efficiency values. Constants that corresponded to the minimum error were chosen to represent the updated tip loss correlation.

Recall equation (1-2): $\quad Y_{TC} = 0.37 \, \frac{c}{h} \left(\frac{k'}{c}\right)^{0.78} \left(\frac{C_L}{s/c}\right)^2 \frac{(\cos\alpha_2)^2}{(\cos\alpha_m)^3}$

3.2.1 Root Mean Square Error (RMSE)

After trying a range of different constants ranging from 0.10 to 0.50 in **equation (1-2)**, the tip loss was used to evaluate total-to-total stage efficiency values, which were compared to those obtained from CFD. The difference between evaluated and CFD

efficiencies values represents the error, which was obtained using the RMSE technique. The constant that corresponded to the minimum error value was chosen to be included in the updated correlation for stepped OD and straight OD configurations.

3.2.1.1   Stepped OD

Total-to-total stage efficiency values were evaluated for 0.10, 0.20, 0.30 and 0.40 constants and the percentage error was plotted against these constants as shown in **Figure 3-19**. The percentage error was evaluated using **equation (3-4)** for 1-, 2-, and 3-fins on the same graph. The constant value was calculated by obtaining the derivative of the second-degree equation shown in **Figure 3-19** and then setting the derivative to zero. This constant value was utilized in the updated correlation for stepped OD configurations. Since the total-to-total stage efficiency values acquired from CFD analysis for both angled and vertical fins were similar, their average was compared to experimental correlations in order to calculate the root mean square error.

$$RMSE = \sqrt{\frac{\sum_1^9\left(Efficiency_{CFD}-Efficiency_{Exp}\right)^2}{9}} \times 100 \tag{3-4}$$

Where $Efficiency_{CFD} = \left(\frac{Eff\cdot Angled + Eff\cdot Vertical}{2}\right)$
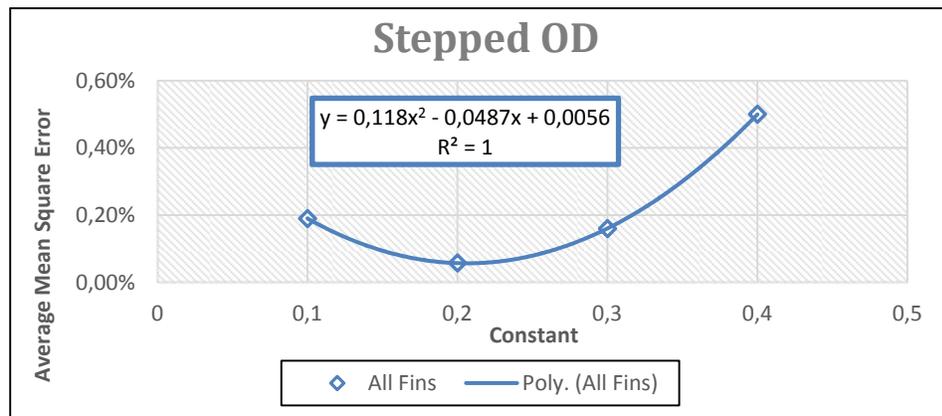
Figure 3-19 RMSE for Stepped OD – (For any # of Fins)

Equation (3-5) shows the equation of the curve in **Figure 3-19**. The derivative of equation (3-5) is $MSE' = 0.236(Constant) - 0.0487$ $(Setting\ MSE' = 0)$ $Constant = \frac{0.0487}{0.236} = 0.206$, which is the updated constant with the least error.

$$MSE = 0.118(Constant)^2 - 0.0487(Constant) + 0.0056 \qquad (3\text{-}5)$$

An additional assessment was performed to verify the accuracy of the 0.206 constant obtained in the new correlation. This was done by checking the error of two more constants within $\pm\ 0.01$ of 0.20 constant (0.19, 0.20, and 0.21) as shown in **Figure 3-20**. There was no need to conduct any further verification with three decimal places since the correlation is likely not more accurate than the value obtained.

Subsequently, the error values were plotted against the constant values, where the constant with the minimum error was chosen, as shown in **Figure 3-20**. A second-degree equation (equation **(3-5)**) was obtained by implementing the best-fit curve of the three points shown in **Figure 3-20**. Setting the derivative of **equation (3-5)** to zero ($y' = 0$) and solving for constant value (x), the minimum error was obtained, which corresponds to the chosen constant value for the new correlation.
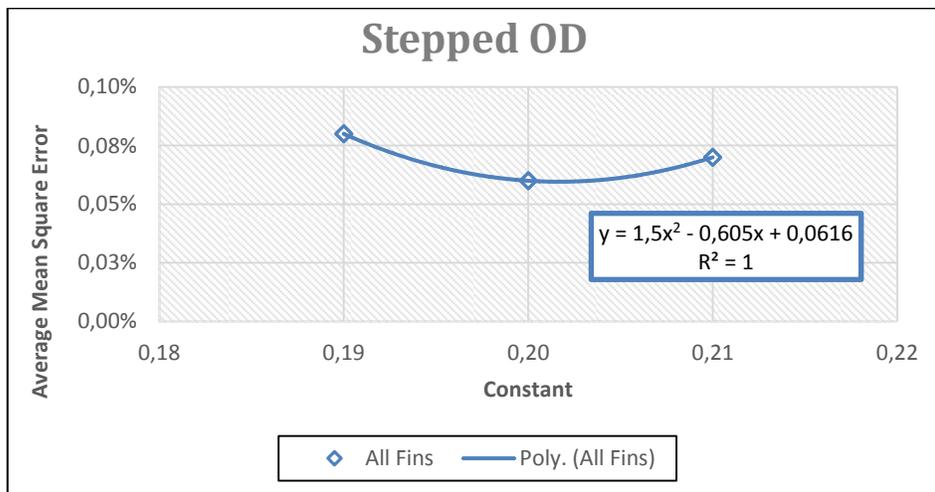
Figure 3-20 RMSE for Stepped OD – 2 Decimal Point (For any # of Fins)

$$MSE = 1.5(Constant)^2 - 0.605(Constant) + 0.0616 \qquad (3\text{-}6)$$

The derivative of equation **(3-5)** is $MSE' = 3(Constant) - 0.605 \; (Setting \; MSE' = 0)$

$$\therefore Constant = \frac{0.605}{3} = 0.20$$

Therefore, an updated correlation for stepped OD configurations was obtained and is presented in **equation (3-7)**. The constant was changed from 0.37 to 0.20 irrespective of fin number and with 0.06% error.

$$\text{Stepped OD (Any \# of fins)} \quad Y_{TC} = 0.20 \; \frac{c}{h}\left(\frac{k'}{c}\right)^{0.78}\left(\frac{C_L}{s/c}\right)^2 \frac{(\cos\alpha_2)^2}{(\cos\alpha_m)^3} \qquad (3\text{-}7)$$

3.2.1.2 Straight OD

The same steps employed in **section 3.2.1.1** were followed for straight OD configurations. The only modification was obtaining a constant for each of the 1-, 2-, and 3-fins separately. First, four constants (between 0.35 and 0.50) were evaluated using Kacker & Okapuu's (1982) tip loss correlation to obtain corresponding stage efficiency values, which were compared to CFD. For example, for a given constant value, percentage error gave the minimum value for the 1-fin configuration but not necessarily for the rest (i.e. 2- and 3-fins). Therefore, it was decided to obtain a constant for each number of fins for the straight OD configurations.

Each configuration with a different number of fins had its own four constants evaluated in the tip loss correlation. Every tip loss evaluation had its corresponding stage efficiency values, which were compared to CFD efficiency values. The percentage error between calculated efficiency values and CFD ones was calculated using RMSE technique. Percentage error was plotted against its corresponding evaluated constants, as shown in **Figure 3-21**.
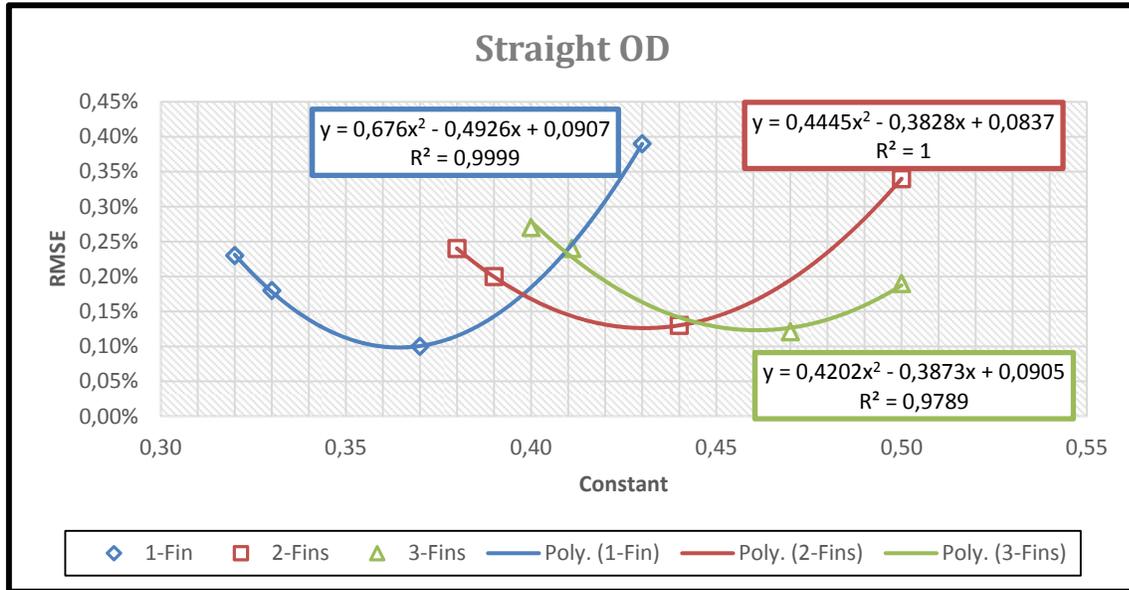
Figure 3-21 RMSE for Straight OD – (1-, 2-, & 3-Fins)

Equations (3-8), **(3-9)**, and **(3-10)** presents the equations of the curves in **Figure 3-21** for 1-, 2-, and 3-fins respectively.

$$\text{MSE}_{1-\text{fin}} = 0.676(\text{Constant})^2 - 0.04926(\text{Constant}) + 0.0907 \qquad (3\text{-}8)$$

$$\text{MSE}_{2-\text{fins}} = 0.4445(\text{Constant})^2 - 0.3828(\text{Constant}) + 0.0837 \qquad (3\text{-}9)$$

$$\text{MSE}_{3-\text{fins}} = 0.4202(\text{Constant})^2 - 0.3873(\text{Constant}) + 0.0905 \qquad (3\text{-}10)$$

Their derivatives are:

$$MSE'_{1-fin} = 1.352(Constant) - 0.4926 \quad (Setting\ MSE'_{1-fin} = 0)$$

$$MSE'_{2-fins} = 0.889(Constant) - 0.3828 \quad (Setting\ MSE'_{2-fins} = 0)$$

$$MSE'_{3-fins} = 0.8404(Constant) - 0.3873 \quad (Setting\ MSE'_{3-fins} = 0)$$

The updated constants that correspond to the minimum percentage error are:

$$Constant_{1-fin} = \frac{0.4926}{1.352} = 0.364$$

$$Constant_{2-fins} = \frac{0.3828}{0.889} = 0.431$$

$$Constant_{3-fins} = \frac{0.3873}{0.8404} = 0.461$$

The next step was to verify the accuracy of the error obtained by choosing constants with up to two-decimal places. This was completed by checking the error of two more constant values within ± 0.01 of each of the 0.36, 0.43 and 0.46 constants, as is shown in **Figure 3-22**. Equations in the figure below were acquired from the best-fit curve for the 1-, 2- and 3-fins that correspond to the constant values of 0.36 (error 0.08%), 0.43 (error 0.10%) and 0.46 (error 0.119%) respectively. These constants were obtained in a similar fashion to the previous step.
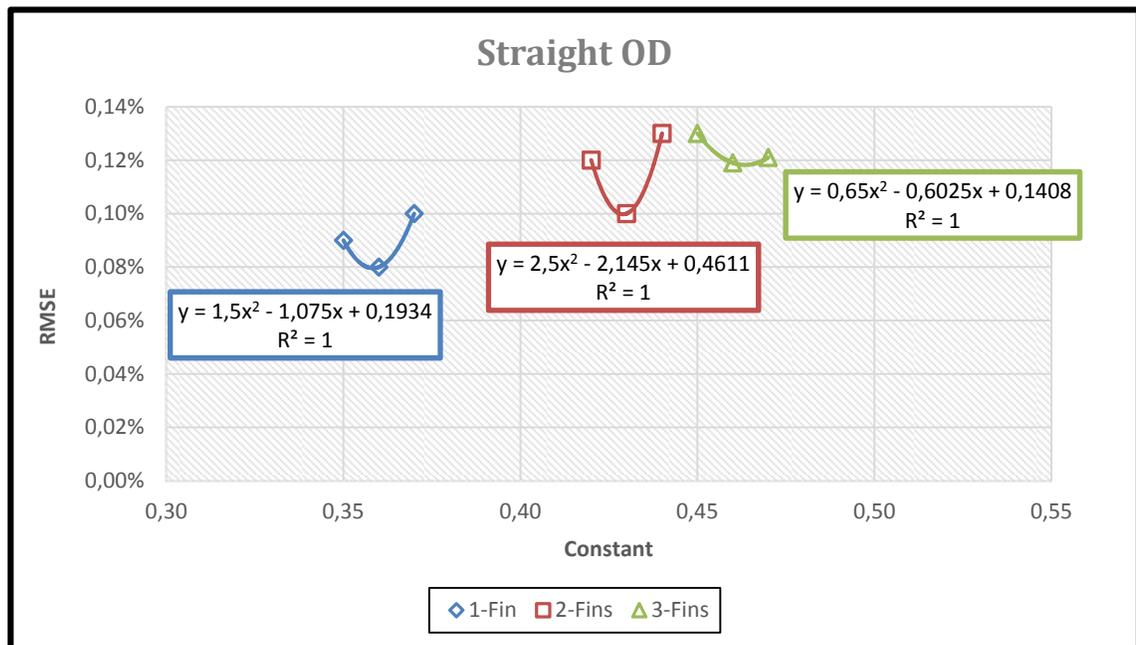
Figure 3-22 RMSE for Straight OD – 2 Decimal Point (1-, 2-, & 3-Fins)

The graphs presented in **Figure 3-22** are exhibited individually throughout **Figure 3-23** to **Figure 3-25** for greater clarity. Finally, the updated correlations for straight OD configurations for 1-, 2-, and 3-fins are shown in **equations (3-11)**, **(3-12)**, **(3-13)** respectively. It is expected to have a lower tip loss as the number of fins increases; and therefore, the constant number should be lower as the number of fins is increased. This was not the case when looking at **equations (3-11)**, **(3-12)**, and **(3-13)**. Thus, it is recommended to modify the $\left(\frac{k'}{c}\right)^{0.78}$ term, which is a function of the number of fins.

Straight OD (1-fin) $\quad Y_{TC} = 0.36 \, \frac{c}{h} \left(\frac{k'}{c}\right)^{0.78} \left(\frac{C_L}{s/c}\right)^2 \frac{(\cos \alpha_2)^2}{(\cos \alpha_m)^3}$ $\qquad$ *(3-11)*

Straight OD (2-fins) $\quad Y_{TC} = 0.43 \, \frac{c}{h} \left(\frac{k'}{c}\right)^{0.78} \left(\frac{C_L}{s/c}\right)^2 \frac{(\cos \alpha_2)^2}{(\cos \alpha_m)^3}$ $\qquad$ *(3-12)*

Straight OD (3-fins) $\quad Y_{TC} = 0.46 \, \frac{c}{h} \left(\frac{k'}{c}\right)^{0.78} \left(\frac{C_L}{s/c}\right)^2 \frac{(\cos \alpha_2)^2}{(\cos \alpha_m)^3}$ $\qquad$ *(3-13)*
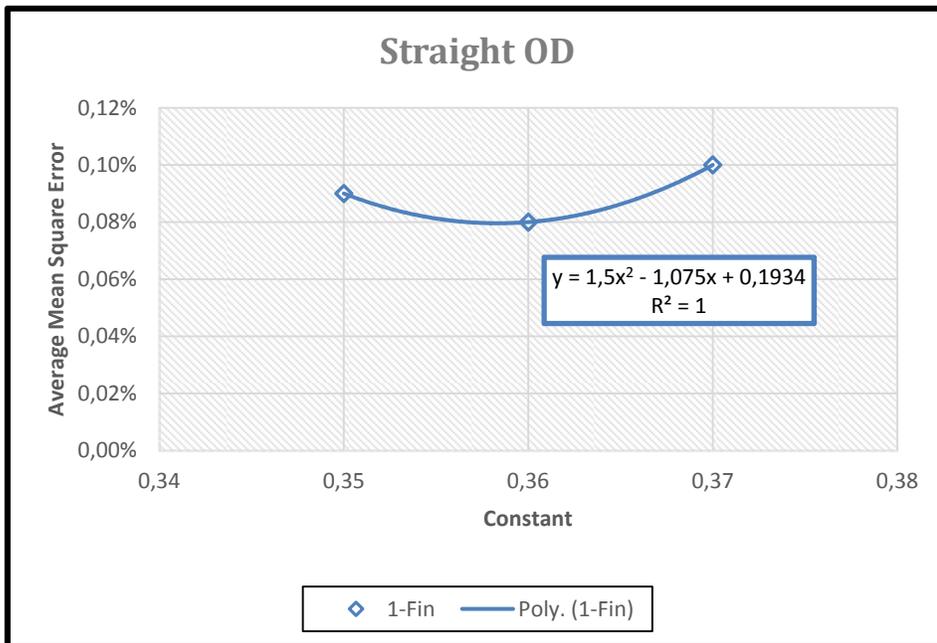
Figure 3-23 RMSE for Straight OD – 2 Decimal Point (1-Fin)
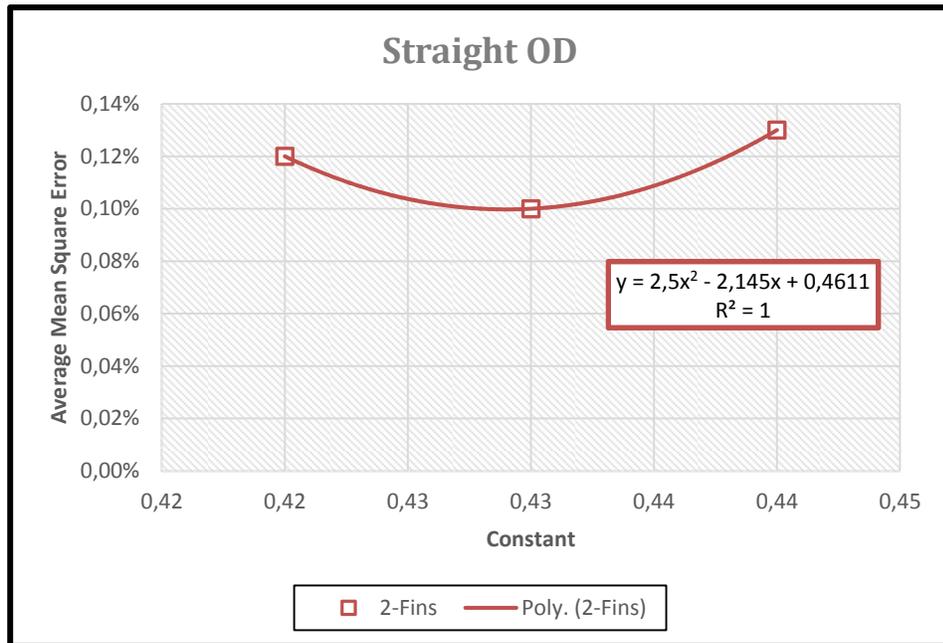
Figure 3-24 RMSE for Straight OD – 2 Decimal Point (2-Fins)
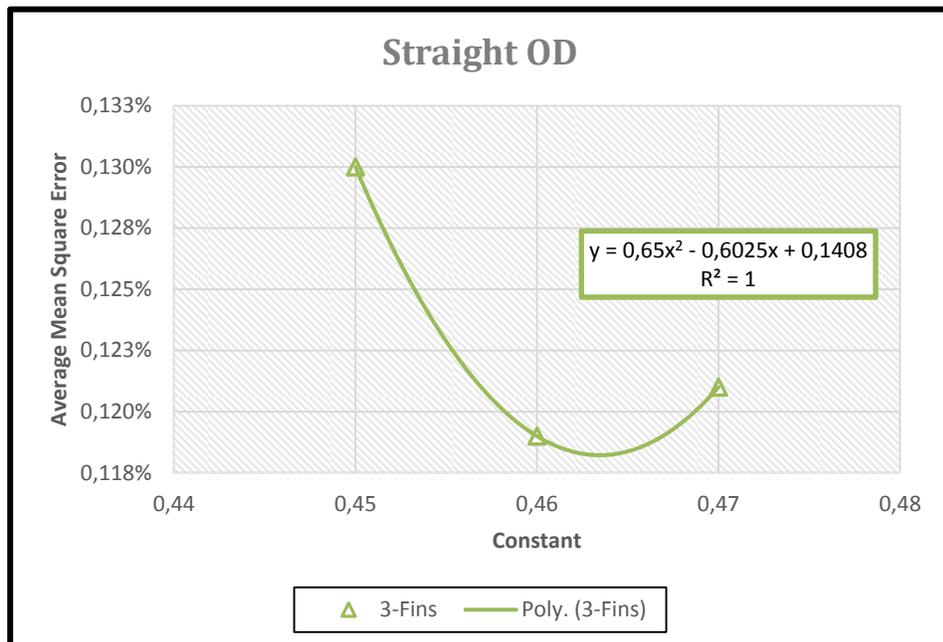
Figure 3-25 RMSE for Straight OD – 2 Decimal Point (3-Fins)

3.2.2 Comparison

Figure 3-26 and **Figure 3-27** show the initial (OLD) and updated (NEW) efficiency values for stepped OD and straight OD configurations respectively. The initial efficiency values were based on the original Kacker & Okapuu's (1982) tip loss correlation and the updated efficiency values were based on the updated Kacker & Okapuu's (1982) tip loss correlation. Clearance-to-span ratios were plotted against change in total-to-total stage efficiency for stepped OD and straight OD configurations with three tip clearance values. Efficiency values of the original (OLD) correlations were presented as solid lines, whereas efficiency values for the updated (NEW) correlations were presented as dashed lines. Efficiencies from CFD results for angled and vertical fins were also included in the same plot.
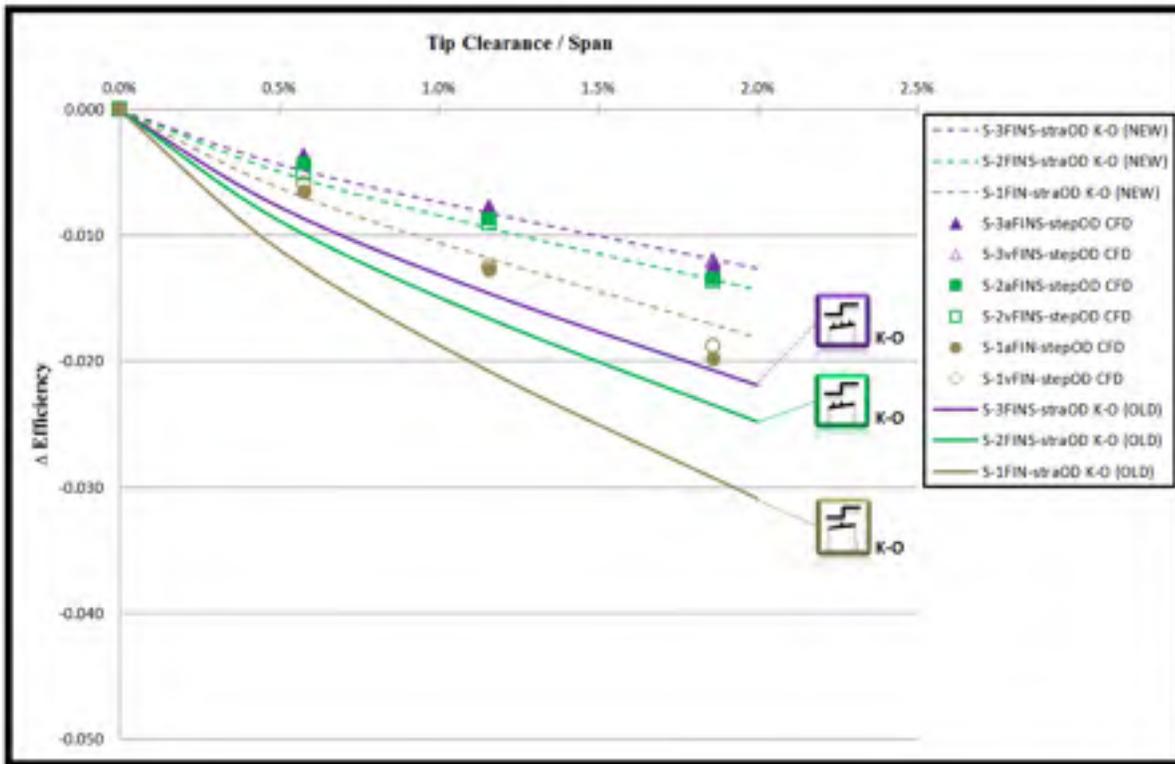
Figure 3-26 Stepped OD - Correlation vs. New Correlations vs. CFD
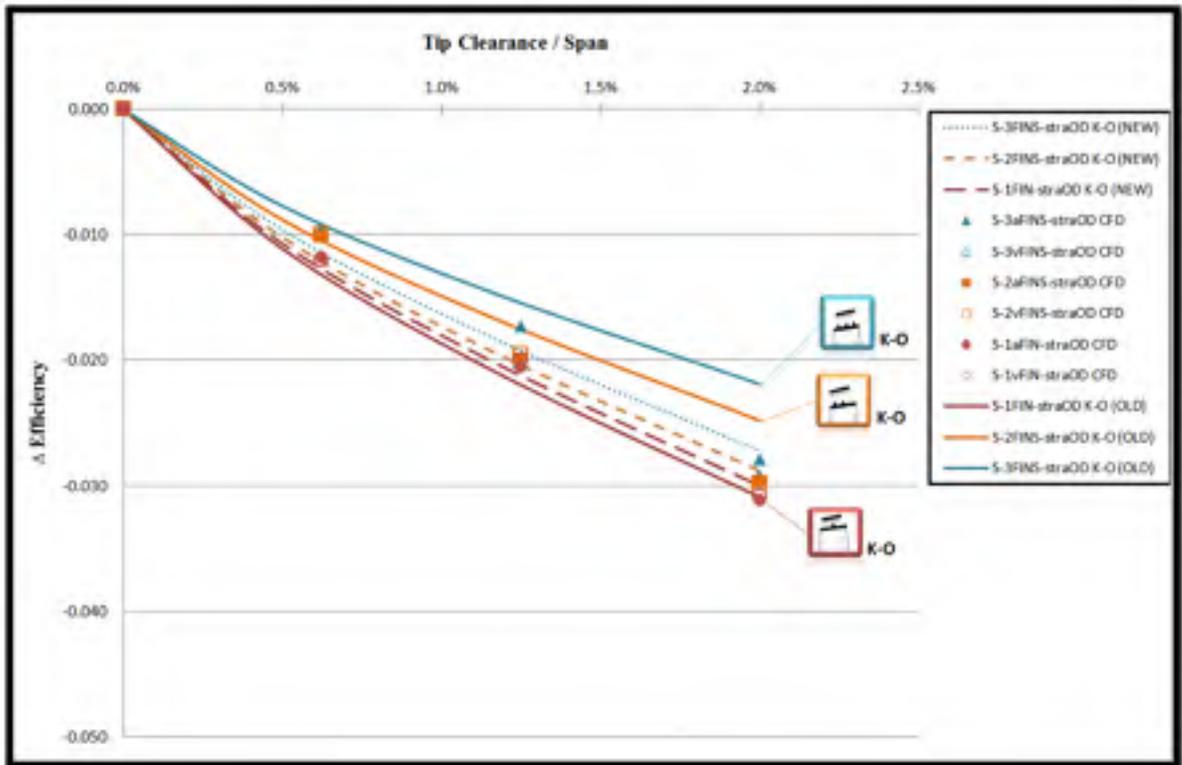
Figure 3-27 Straight OD - Correlations vs. New Correlation vs. CFD

3.3   Summary

Results showed that configurations with stepped OD had lower mass flow at blade tip area than with straight OD. Stepped OD configurations exhibited more consistency in terms of mass flow and efficiency when compared to those with straight OD. In addition, when increasing the number of fins on stepped OD configurations, CFD results showed a smoother flow at the blade tip area than with straight OD configurations for a given tip clearance space. Moreover, a minor difference was noted when comparing vertical to angled fins for stepped and straight OD configurations.

For stepped OD configurations, it was found that when evaluating 0.20 (0.06% error) for the constant in Kacker & Okappu's (1982) tip loss correlation, (**equation 1-2**) it gave the closest total-to-total stage efficiency values with respect to CFD results for any number of

fins. Whereas for straight OD configurations, three different constants were obtained to match the total-to-total stage efficiency values with respect to CFD results. The updated constants for straight OD configurations were 0.36 (error 0.08%), 0.43 (error 0.10%) and 0.46 (error 0.119%), which correspond to 1-, 2-, and 3-fins respectively.

CONCLUSION AND FUTURE WORK

Tip clearance loss prediction is an integral topic in understanding and minimizing losses in gas turbines to increase its overall efficiency. An experimental study by Kacker & Okapuu (1982) devised an experimental-based correlation to predict tip clearance loss. A previous study by Stocker (1978) claimed that angled fins function as an ideal tip clearance seal when compared to vertical fins, and stated that fins with stepped OD had less tip clearance loss than those with straight OD.

The objective of this study was to improve tip loss correlation of shrouded blades, and to investigate the tip leakage of several blade tip configurations of a one-stage (2nd stage) passage in an axial power turbine. Moreover, updated tip loss correlations were extracted for stepped OD and straight OD configurations with one, two and three fins based on a numerical simulation. In addition, the aim was to comprehend the flow behaviour, for different configurations with different fin (angled, vertical) and outer diameter (stepped, straight) types, in the area wherein interaction between casing and blade tip occurs. CFD simulations were performed because it is a cost effective method and its ease in observing flow properties at any region of the simulated model.

Study Procedure Summary

One stage of a power turbine was simulated in this study with twelve different configurations were analyzed; each had three distinct tip clearances of .015 in, .030 in and .048 in. An additional model was created with zero clearance for reference. Therefore, a total of 37 models were created, meshed and simulated. Each configuration differed from another with respect to changes in the outer diameter (i.e., step and straight), number of fins (i.e., one, two and three), and fin type (i.e., angled and vertical) at the blade tip area. The breakdown of these twelve configurations can be represented as six stepped OD (3-angled fins and 3-

vertical fins) and six straight OD (3-angled fins and 3-vertical fins). A mesh study was performed on one model where seven different meshes were created; due to the available run time to complete the project, a relatively coarse mesh size was chosen. The same vane model, mesh sizes, and boundary conditions were utilized for all configurations. Boundary conditions were applied at vane inlet (e.g., total pressure, total temperature, and flow inlet angle), blade exit (e.g., static pressure) and at inner walls (e.g., smooth walls). The K$-\omega$ shear stress transport (SST) model was used to run CFD simulation. Stage efficiencies calculated from CFD results were used to compare different geometries such as stepped and straight OD configurations, angled and vertical fins, and addition of number of fins (i.e., one, two and three fins). Comparisons were conducted by plotting the change in total-to-total stage efficiency values of all configurations against their corresponding clearance-to-span ratios. In addition, total-to-total stage efficiencies were calculated using tip loss experimental correlations and were compared to CFD stage efficiencies for both stepped and vertical OD configurations with one, two and three fins.

Overview of Study Findings

The primary finding of this paper revealed that the tip loss experimental correlation presented in Kacker & Okapuu's (1982) tip loss correlation underestimated stage efficiency values obtained for stepped OD configuration when compared to CFD stage efficiency values. The total-to-total stage efficiency values obtained from the mean-line using Kacker & Okapuu's (1982) tip loss correlation showed different results when compared to total-to-total stage efficiency values from CFD. The constant found in Kacker & Okapuu's (1982) tip loss correlation was modified from 0.37 to 0.20 to align those efficiency values obtained from CFD simulation with a 0.06% error. On the other hand, obtaining one updated correlation for straight OD configurations for any number of fins was not possible since stage efficiency results did not aligned properly. Nevertheless, it was possible to obtain three-updated correlations for straight OD configurations for each number of fins. The 0.37 constant was

modified to 0.36, 0.43 and 0.46 for 1-, 2-, and 3-fins configurations with 0.08%, 0.10%, and 0.12% error respectively.

Moreover, this study uncovered that shrouded blades with straight OD configurations had lower efficiencies than shrouded blades with stepped OD. This difference was because configurations with stepped OD had a lower mass flow at blade tip than straight OD. Moreover, velocity streamlines from CFD showed that flow disturbance was more prominent in the straight OD tip area. When comparing angled and vertical fins (i.e., stepped OD with 2-angled-fins and stepped OD with 2-vertical-fins configurations), CFD results showed a minor difference in terms of mass flow at blade tip area and hence, efficiency values did not show a great difference. In terms of tip mass flow, with the addition of fins to the shroud, flow resistance increased; the 1-fin shroud had the least tip mass flow, followed by the 2-fin and 3-fin shrouds. This pattern was observed for both straight and stepped OD configurations. It was concluded that higher efficiencies were to be obtained for any clearance value of configurations with stepped OD and a larger number of fins.

Implications

This study successfully aligned Kacker & Okapuu's (1982) tip-clearance-loss correlation (experimental-based) of a shrouded blade of a power turbine based on CFD analysis. This improvement suggests that Kacker & Okapuu's (1982) tip loss correlation closely predicted tip loss but it required minor adjustment, which was achieved by modifying the constants in the correlation. Improvement of the tip-clearance loss correlation (experimental-based) will empower the PDDS tool currently used by industry to possess tip-loss predictions of turbine blades at a preliminary design stage. This suggests that greater confidence can be placed into this particular tool by those using it in the aerospace industry, which will likely contribute to increased overall efficacy of practice.

Stepped OD configurations with angled fins did not exhibit a significant difference in terms of mass flow at blade tip than stepped OD configurations with vertical fins. Total-to-

total stage efficiency values for all configurations and different clearances did not show a significant difference between angled and vertical fins. In response to these findings, more attention in research needs to be focused on vertical fin design when examining tip clearance loss. The vertical fin design used in this study possessed some differences (i.e., tapered edges) when compared to those used by Stocker (1978) (i.e., pointed tips), as shown in **Figure 1**. This suggests that fin design could have an impact on tip-loss evaluation and thus should be examined in greater detail in future research.
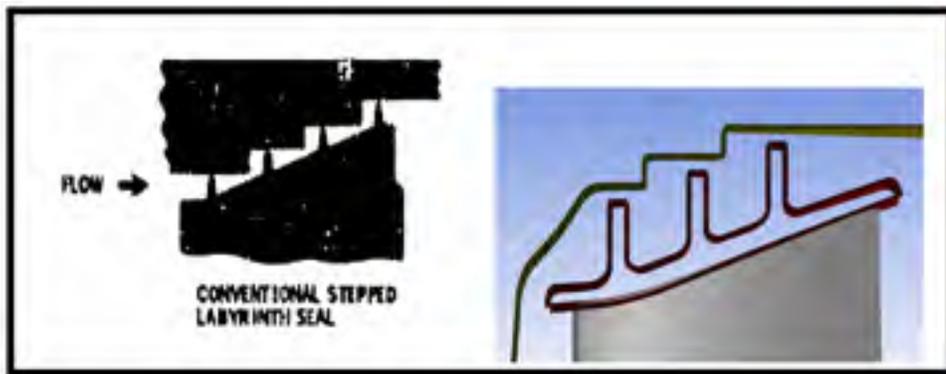
Figure 1 Vertical Fin – Stocker (1978) [left] and current study fin [right]

This study confirmed and validated previous findings wherein stepped OD with angled fins were found to have less tip loss than straight OD with vertical fins (Stocker, 1978). This finding has the following implications in regards to the aerospace industry:

- Decrease of tip leakage losses in turbine, which will contribute to an increase in overall efficiency.
- Encourage industry to continue using and work towards obtaining an optimal design for stepped OD configurations on turbine blades.
- Provides the basis to perform blade-tip-loss simulation on: *(i)* all stages of the power turbine, *(ii)* and power turbine of bigger engines.

- Offers an opportunity to develop a long term "CFD (vs experimental) based correlation.

Limitations

As mentioned in the mesh sensitivity study of this paper, the mesh chosen to perform the CFD analysis was not performed with the finest mesh (Mesh 1) obtained in the mesh sensitivity study. This was due to the run time available to complete this study. Given that all configurations had the same mesh sizes, it was assumed that difference in results were due to the change of blade tip geometry.

It would have been ideal to take more time to acquire a better-quality mesh, which would have increased the accuracy of the results. Performing analysis over time would have enabled for the comparison of these results with those acquired in this study. Such a comparison would have indicated whether there was a significant difference between the better-quality mesh and the results acquired in this study, which would have identified the mesh quality needed to check for accuracy of efficiency values. It is important to note that the difference in the $\Delta\eta$ between the chosen mesh (Mesh 4) and the fine mesh (Mesh 1) is 0.08% or 0.0008, which would not drastically affect the results obtained by the current study.

Moreover, the RANS Models could be over dissipative in such complex flow, and CFD results were not experimentally validated against same blade models created in this study.

Future Research

A recommendation for subsequent research would be to recreate the mesh and CFD simulation of all configurations with a fine mesh and compare results with those acquired in this study. This would require approximately 16 working hours for each mesh model and approximately 6 hours of run-time for each CFD simulation. In addition, many different

aspects of fin designs could be investigated to obtain an optimal design; such as, simulate different clearance-to-fin ratios, establish a fixed distance between fins for 2- and 3-fin configurations, and distance between fin tip and OD step. For example, as was mentioned by Gamal and Vance (2008), doubling the fin thickness resulted in a decrease in flow leakage by 20%. Furthermore, a new correlation for straight OD configurations could be acquired by modifying one or both constants in the $\left(\frac{k}{c \times (number\ of\ seals)^{0.42}} \right)^{0.78}$ term, which can be found in Kacker & Okapuu's (1982) tip loss correlation. Therefore, it can be suggested that modifying the constants 0.42 and/or 0.78 would be an ideal adaptation to acquire one new correlation for straight OD configurations for a given number of fins. Furthermore, **equations (3-11)**, **(3-12)**, and **(3-13)** showed an increasing constant value as the number of fins was increased, which means that the 3-fin configuration has a higher tip leakage. This is not the case. **Equations (3-11)**, **(3-12)**, and **(3-13)** are not recommended to evaluate the tip clearance loss for straight OD configurations.

Subsequent studies could also provide the opportunity for improvement of tip loss evaluation of turbine blades. Kacker & Okapuu's (1982) tip loss correlation could be evaluated in a similar manner to that performed in this study on different blade and blade tip designs. Moreover, comparison between Kacker & Okapuu's (1982) tip loss correlation and the updated correlations presented in this study could be conducted in order to verify and validate the accuracy of the updated tip loss correlations.

LIST OF REFERENCES

ANSYS. (2013). *ANSYS Guide.* Canosnsburg, PA, USA.

Bardina, J., Huang, P., & Coakley, T. (1997). *Turbulence Modeling Validation, Testing and Development.*

Camci, C., Dey, D., & Kavurmacioglu, L. (2005). Aerodynamics of Tip Leakage Flows Near Partial Squealer Rim in an Axial Flow Turbine Stage. *Journal of Turbomachinery, 127*, 14-24. doi:10.1115/1.1791279.

Collins, D. (2007). *The Effects of Wear on Abradable Honeycomb Labyrinth Seals.* Cranfield University, Power, Propulsion & Aerospace Engineering. Retrieved 10 10, 2015.

Gamal, A. J., & Vance, J. M. (2008). Labyrinth Seal Leakage Test: Tooth Profile, Tooth Thickness, and Eccentricity Effects. *Engineering for Gas Turbines and Powers, 130*, 11. doi:10.1115/1.2771571.

Han, J.-C., Dutta, S., & Ekkad, S. (2013). *Gas Turbine Transfer and Cooling Technology.* Boca Raton: CRC PRess.

Hanimann, L., Mangani, L., Casartelli, E., Monkulys, T., & Mauri, S. (2014). Development of a Novel Mixing Plane Interface Using a Fully Implicit Averaging for Stage Analysis. *Journal of Turbomachinery, 136*(8).

Huang, A. C., Greitzer, E. M., Tan, C. S., Clemens, E. F., Gegg, S. G., & Turner, E. R. (2013). Blade Loading Effects on Axial Turbine Tip Leakage Vortex Dynamics and Loss. *Jurnal of Turbomachinery, 135*, 11. doi:10.1115/1.4007832.

Intaratep, N. (2006). *Formation and development of the tip leakage vortex in a simulated axial compressor with unsteady inflow.* Virginia Polytechnic Institute, Aerospace Engineering. Ann Arbor: ProQuest. Retrieved February 18, 2015, from < http://search.proquest.com/docview/304968020?accountid=27231 >.

Kacker, S. C., & Okapuu, U. (1982). A Mean Line Prediction Method for Axial Flow Turbine Efficiency. *Journal of Engineering for Power, Vol. 104*, 111-119.

Komotori, K., & Miyake, K. (1977). Leakage Characteristics of Labyrinth Seals With High Rotating Speed. *Tokyo Joint Gas Turbine Congress*, 371-380.

Li, J., Qiu, B., & Feng, Z. (2012). Experimental and Numerical Investigations on the Leakage Flow Characteristics of the Labyrinth Brush Seal. *Engineering for Gas Turbines and Power, 134*, 1-9. doi:10.1115/1.4007062.

Mangani, L., Casartelli, E., Wild, M., & Spyrou, N. (2014). Assessment of an implicit mixing plane approach for pump-turbine applications. *Earth and Enivronmental Science, 22*(2), 022003.

Moustapha, H., Zelesky, M. F., Banies, N. C., & Kapikse, D. (2003). *Axial and Radial Turbines.* White River Junction, Vermont, USA: Concpets NREC.

Pfau, A. (2003). *Loss Mechanisms in Labyrinth Seals of Shrouded Axial Turbines.* Zurich.

Saravanamuttoo, H., Rogers, G., Cohen, H., & Straznicky, P. (2009). *Gas Turbine Theory* (Sixth Edition ed.). Harlow, Essex, England: Pearson Education Limited.

Shavalikul, A. (2009). *A Time Accurate Prediction Of The Viscous Flow In A Trubine Stage Including A Rotor In Motion.* The Pennsylvania State University, Aerospace Engineering, Philadelphia. Retrieved January 14, 2015 from < http://search.proquest.com/docview/304984061?accountid=27231 >.

Stocker, H. L. (1978). *Determining And Improving Labyrinth Seal Performance In Current And Advanced High Performance Gas Turbines.* General Motors Corporations, Flow Systems Group. Indianapolis: Internal Aerodynamics Detroit Dioesel Allison. Retrieved 05 2015.

Szymański, A., Dykas, S., Wróblewski, W., & Rulik, S. (2014). Investigation of the tip-leakage losses in turbine axial stages. *Journal of Physics, 530*. doi:10.1088/1742-6596/530/1/012033.

Tallman, J. A. (2002). *A computational study of tip desensitization in axial flow turbines.* Doctor of Philosophy , The Pennsylvania State University, Mechanical Engineering, Philadelphia. Retrieved January 15, 2015 from < http://search.proquest.com/docview/305530684?accountid=27231 >.

Vermes, G. (1961). A Fluid Mechanics Approach to the Labyrinth Seal Leakage Problem. *Journal of Engineering for Power*, 161-169.

Wang, D. (2014). An Improved Mixing-Plane method for Analyzing Steady Flow through Multiple-Blade-Row Turbomachines. *Journal of Turbomachinery, 136*(8).

Yoon, S., Curtis, E., Denton, J., & Longley, J. (2014). The Effect of Clearance on Shrouded and Unshrouded Turbines at Two levels of Reaction. *Journal of Turbomachinery, 136*, 9. doi:10.1115/1.4023942.

Zhang, W.-F., Yang, J.-G., Li, C., & Tian, Y.-W. (2014). Comparison of leakage performance and fluid-induced force of turbine tip labyrinth seal and a new kind of radial annular seal. *Computers & Fluids, 105*, 125-137. Retrieved January 14, 2015, from < http://www.sciencedirect.com/science/article/pii/S0045793014003478 >.

Zhou, C., Hodson, H., Tibbott, I., & Stokes, M. (2013). Effects of Winglet Geometry on the Aerodynamic Performance of Tip Leakage Flow in a Turbine Casade. *Journal of Turbomachinery, 135*, 10. doi:10.1115/1.4007831.